

RESEARCH

Open Access



Non-orthogonal multiple access in full-duplex-based coordinated direct and relay transmission (CDRT) system: performance analysis and optimization

Aswathi V* and Babu A V

Abstract

This paper considers non-orthogonal multiple access (NOMA)-based coordinated direct and relay transmission (CDRT) system, where the base station (BS) directly communicates with the nearby users while it requires the help of a dedicated relay to communicate with the cell-edge users. We derive exact closed form expression for the outage probabilities experienced by the downlink users and the system outage probability of the considered CDRT network with full-duplex relaying (FDR) technique. Further, we derive approximate closed form expressions for the ergodic rates achieved by the users. The channel of all the links experience Nakagami fading distribution and the analysis takes into account the residual interference generated due to the imperfect successive interference cancelation (I-SIC) technique. We provide numerical and simulation results to identify the impact of key system parameters on the outage and ergodic rate performance of the users and the system outage performance. The outage and ergodic rate performance of users in the considered FDR-based NOMA-CDRT system has been observed to be significantly improved compared to a FDR-based OMA (orthogonal multiple access)-CDRT system. It is observed that random selection of NOMA power allocation coefficients at the BS leads to higher outage for the near users compared to the far users. We determine numerical results for the NOMA power allocation coefficient that leads to equal outage performance for both the users. Finally, we derive analytical expression for the optimal power allocation (OPA) coefficient at the BS that minimizes the system outage probability. Through extensive numerical and simulation studies, we establish that OPA can lead to significant reduction of system outage probability compared to random selection of power allocation coefficients at the BS.

Keywords: Non-orthogonal multiple access, Coordinated direct and relay transmission, Full duplex, Nakagami, Optimal power allocation

1 Introduction

Recently non-orthogonal multiple access (NOMA) has been identified as an effective multiple access technique to improve the spectrum efficiency in the fifth generation (5G) wireless networks. NOMA technique allows multiple users to coexist and share the same time-frequency resource block via power domain multiplexing mechanism [1, 2]. In this case, a NOMA enabled BS will apply the superposition coding technique to combine

multiple user's signals with distinct power levels, while the receivers use the successive interference cancelation (SIC) technique to decode the message. In a cooperative NOMA system, strong users (i.e., users experiencing better channel conditions) act as relays for delivering the message to weak users in the system [3]. In NOMA-based CDRT systems, the BS directly communicates with the nearby users while it requires the help of a dedicated relay to communicate with the far users [4]. The spectral efficiency of the system can be improved by operating the relay in the full-duplex mode that enables it to carry out simultaneous reception and transmission in the same frequency resource. However, in-band FDR technique leads

*Correspondence: aswathi481@gmail.com
Electronics and Communication Engineering Department, National Institute of Technology, Calicut, Kerala, India

to the generation of self-interference (SI) at the relay node, which is induced from its transmitter to the receive section [5]. Even though, the effect of SI can be mitigated by sophisticated interference suppression techniques, the relay node will still be affected by residual self-interference (RSI), which proportionally grows with the used transmit power [6].

The focus of the current work is on the performance analysis of NOMA-based CDRT system that employs FDR technique. The performance of cooperative NOMA system with half duplex relaying (HDR) has been analyzed thoroughly in the literature (e.g., [7–14] and references therein). The performance of cooperative NOMA-based CDRT has also been analyzed in the literature [4, 15–17]. In [4], the authors have considered the application of NOMA in two-user HDR based CDRT system and analyzed the outage and ergodic sum rate performance. In [15], the authors have considered the application of uplink NOMA in HDR-based CDRT system. The ergodic sum capacity of the system has been analyzed under both perfect and imperfect SIC conditions. In [16], the authors have analyzed the outage and ergodic rate performance of the near and the far users in HDR-based NOMA-CDRT system, where an energy harvesting relay has been employed to assist the BS for delivering message to the far user. The authors of [17] have considered HDR-based NOMA-CDRT system with two cell-center users (CCUs) and a cell-edge user (CEU), which is assisted by a relay. Notice that all the above papers consider the performance evaluation of HDR-based NOMA-CDRT system.

In downlink cooperative NOMA system, the strong users will first decode the signal corresponding to the weak users from the received NOMA signal. They will then implement the SIC technique to cancel the signal corresponding to the weak users, before decoding their own symbol [18]. Imperfect SIC (I-SIC) will lead to the generation of residual interference at the near users. Recently, the performance of FDR-based cooperative NOMA system has been investigated extensively in the literature [18–26]. In [18, 19], the authors have considered a cooperative NOMA system with half/full duplex relaying and evaluated the performance of the system in terms of outage probability, ergodic rate, and energy efficiency, under perfect SIC (P-SIC) conditions. The impact of relay selection strategy on the performance of cooperative NOMA system has been analyzed in [20], assuming that the relays can operate in either full-duplex (FD) or half-duplex (HD) mode. In [21], the authors have analyzed the outage probability performance of downlink cooperative NOMA system where the relay harvests energy from source, assuming P-SIC condition. In [22], the authors have analyzed the outage and ergodic rate performance of FDR-based NOMA-CDRT system in Rayleigh fading channels, assuming P-SIC. The outage and ergodic sum

rate performance of FDR-based NOMA-CDRT system has been analyzed in [23], in the presence of Nakagami fading channels under P-SIC condition. Further, to simplify the analysis, the RSI at the relay node has been modeled as a Gaussian random variable in [23]. The outage performance of FD-based NOMA-CDRT system has been analyzed in [24, 25] as well, assuming Nakagami fading channels under I-SIC; however, the evaluation of ergodic rates and ergodic sum rate have been ignored. In [26], the authors have considered a cooperative NOMA system, where a CCU is paired with multiple CEUs on a time sharing basis to improve the spectrum efficiency. The authors have established that the proposed system can achieve significant increase of ergodic sum rate as compared to existing benchmark schemes.

In this paper, we derive closed form expressions for the outage probabilities experienced by the users and the system outage probability of FDR-based NOMA-CDRT system assuming the links to experience Nakagami fading, under the realistic assumption of I-SIC. Further, we derive approximate closed form expressions for the ergodic rates achieved by the users in the system under I-SIC. A single-cell downlink NOMA-CDRT system is considered consisting of a BS, a cell-centric (i.e., near) user, a cell-edge (i.e., far) user, and a relay which operates in the FD mode and assists the BS to deliver information to the far user. The major contributions of this paper are outlined as follows:

- Closed-form expressions are derived for the outage probabilities experienced by the users in FDR-based NOMA-CDRT system, under the realistic assumption of I-SIC. An analytical expression for the system outage probability is also presented. Approximate closed-form expressions for the ergodic rates achieved by the users are derived, assuming I-SIC. Numerical results for the outage and ergodic rate performance of the users are presented. Further, numerical results for the system outage and ergodic sum rate performance of the considered FDR-based NOMA-CDRT network are also presented. Analytical results are corroborated by Monte Carlo-based extensive simulation studies.
- In the considered FDR/HDR-based NOMA-CDRT system, random selection of NOMA power allocation coefficient at the BS leads to poor outage performance for the near user compared to the far user. We present insights on selection of NOMA power allocation coefficient that provides equal outage performance for both the near and the far users.
- The performance of the users in FDR-based NOMA-CDRT system has been compared against that is perceived in a CDRT system which use conventional

OMA technique based on time division multiple access (TDMA) scheme.

- We derive analytical expression for the OPA factor at the BS that minimizes the system outage probability of FDR-NOMA-CDRT system. We evaluate the percentage improvement in system outage under the OPA compared to random (i.e., non-optimal) power allocation (RPA) at the BS. With the help of numerical and simulation investigations, we establish that the system outage improves significantly under the OPA strategy.

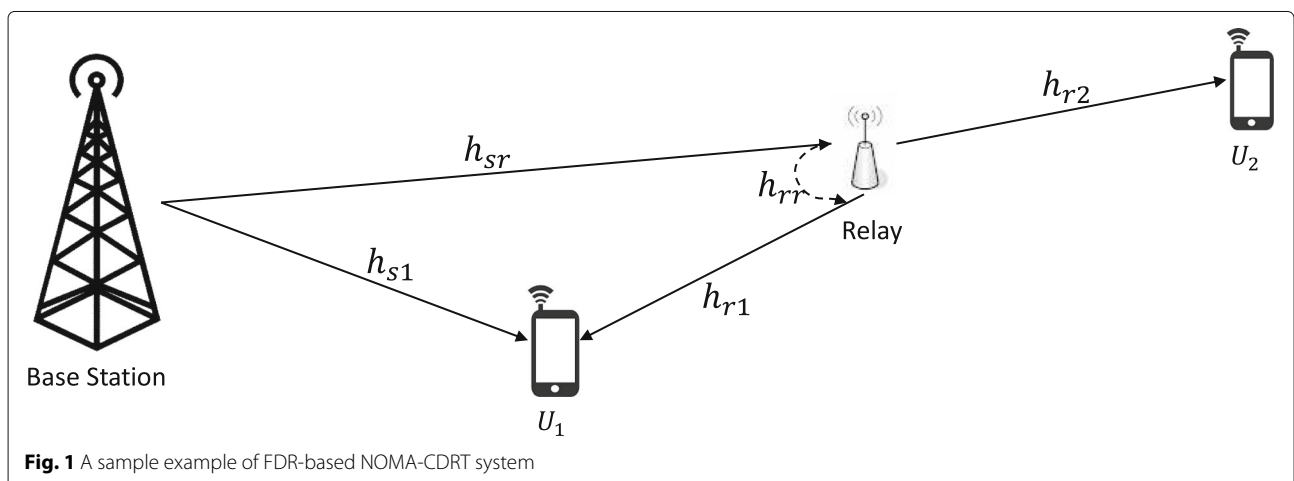
Notice that the system model (i.e., the network and signal model) considered in our paper is similar to that considered in [22–25]. In [22, 23], the authors have assumed P-SIC, while the works reported in [24, 25] have considered I-SIC condition. Further, the authors of [22] have assumed Rayleigh fading while Nakagami fading model was used in [23], where the RSI was approximated as a Gaussian random variable. Even though I-SIC condition was assumed in [24, 25], evaluation of ergodic rates of the users and the ergodic sum rate of the system under the realistic assumption of I-SIC have not appeared in these papers. Moreover, according to our best knowledge, the evaluation of the system outage probability of the considered FD-based NOMA-CDRT network and the investigation of OPA that minimizes the system outage probability have not appeared in the literature so far. The rest of the paper is organized as follows. The system model/experimental used in the paper are summarized in Section 2. Section 3 describes the system model while the derivation of outage probability and ergodic rates are presented in Section 4. Section 5 considers minimization of system outage probability and derives analytical expressions for the OPA to meet the desired objective. The numerical and simulation results are described in Section 6. Finally, the paper is concluded in Section 7.

2 Methods/experimental

In this work, we have considered a CDRT system where the BS delivers message to downlink users using NOMA technique. From a practical perspective, the considered system resembles the conventional relay-based cellular wireless communication scenario. To improve the spectral efficiency of the NOMA-CDRT system, the relay node is assumed to operate in FD mode. The reliability of downlink communication system is analyzed in terms of outage probabilities. Further, the achievable ergodic rates of downlink users are also analyzed. We have used realistic channel model, basics of digital communication principles, and probability theory to analyze the performance of the considered FDR-based NOMA-CDRT system. Furthermore, OPA factor at the BS for improving the system outage performance is investigated. Experimental investigations are carried out using Monte Carlo techniques to validate the analytical findings.

3 System model and preliminary details

The downlink cooperative FDR-based NOMA-CDRT system shown in Fig. 1 is considered where user 1 (U_1) happens to be the near user and user 2 (U_2) is the far user. The BS has direct communication link to U_1 while it is assumed that, due to heavy shadow fading, the direct communication link between BS and U_2 is absent. Accordingly, the BS employs a dedicated FD-based relay (R) to deliver the messages to U_2 . We consider that R can operate as a DF relay. Let $\{h_{ij}, i \in (s, r), j \in (r, 1, 2)\}$ be the channel coefficients corresponding to the links between nodes i and j . We assume the links to experience independent non-identically distributed (i.n.i.d.) Nakagami fading with shape parameter m_{ij} and mean power $\mathbb{E}[|h_{ij}|^2] = \pi_{ij}$. Accordingly, $|h_{ij}|^2$ have Gamma distribution with shape parameter m_{ij} and scale parameter $\beta_{ij} = \pi_{ij}/m_{ij}$. The probability density function (PDF) of $|h_{ij}|$ is given by [27]:



$$f_{|h_{ij}|}(x) = \left(\frac{m_{ij}}{\pi_{ij}} \right)^{m_{ij}} \frac{(2x)^{m_{ij}-1}}{\Gamma(m_{ij})} e^{-\frac{m_{ij}}{\pi_{ij}}x^2} \quad (1)$$

where $\Gamma(\cdot)$ is the Gamma function. The CDF and PDF of $|h_{ij}|^2$ are given by [27]:

$$F_{|h_{ij}|^2}(x) = 1 - e^{-\frac{x}{\beta_{ij}}} \sum_{j=0}^{m_{ij}-1} \frac{\left(\frac{x}{\beta_{ij}}\right)^j}{j!} \quad (2a)$$

$$f_{|h_{ij}|^2}(y) = (\beta_{ij})^{-m_{ij}} \frac{y^{m_{ij}-1}}{\Gamma(m_{ij})} e^{-\frac{y}{\beta_{ij}}} \quad (2b)$$

Notice that (2a) assumes m_{ij} to take integer values only.

We assume $\pi_{ij} = \left(\frac{d_{ij}}{d_0}\right)^{-n}$ where n is the path loss exponent; d_{ij} is the distance between nodes i and j ; $i \in (s, r)$, $j \in (1, r, 2)$; and d_0 is the reference distance (in the far-field region of the transmitting node). Further, it is assumed that all the links experience frequency flat block fading. Furthermore, all the nodes in the network experience additive white Gaussian noise (AWGN) of equal variance σ^2 .

When R operates in the FD mode, it suffers from strong SI which is induced from its transmitter to the receiver side. It is assumed that all the nodes in the network shown in Fig. 1 (except R) use single antenna while R uses two directional antennas. This enables R to perform simultaneous transmission and reception in the same frequency band. Use of directional antennas at R reduces the effect of SI to a great extent [5, 6]. According to the recent literature on state-of-art methods for SI suppression/cancellation, multiple techniques have to be successively applied to the SI signal on top of one another to make the SI cancellation effective. Recently, many techniques have been reported for the mitigation of SI present in FDR systems such as (i) physical isolation, (ii) analog cancellation, and (iii) digital cancellation. Physical isolation techniques attempt to physically prevent the transmitted signal from reaching the receiver-end of the FD node by employing different approaches [28–30] such as (i) placing shielding plates between the transmitter and receiver sections, (ii) using directional transmit antennas with nulls spatially projected at the receive antennas, and (iii) using orthogonally polarized transmit and receive antennas.

Even though these techniques significantly reduce the SI, additional mitigation is usually required due to the overwhelming strength of the interfering signal. Although originally believed to be impractical, FD wireless operation has been recently shown to be feasible through the use of novel techniques for SI isolation and cancellation [31–36]. In spite of the advancements made on the design of SI cancellation methods, it has been well established that SI cannot be canceled completely, and thus, residual self-interference (RSI) would always be present at the FDR nodes. Experimental studies reported in

[31, 37] have suggested that the RSI channel can be modeled as a fading channel. However, the probability distribution of the RSI fading channel differs according to the isolation/cancellation technique employed [31], where the PDF has been modeled as Rician with appropriate K (i.e., Rician factor) values. According to the results in [37], when a strong passive suppression is employed, the line-of-sight (LOS) component of SI is sufficiently suppressed and the PDF becomes Rayleigh. Research work reported in [38, 39] have used Nakagami fading model for the RSI channel. Since Nakagami fading model can represent both Rayleigh and Rician cases, we assume the RSI channel to undergo Nakagami fading. Let h_{rr} be the channel coefficient corresponding to the RSI channel; we assume $|h_{rr}|$ to follow Nakagami- m fading with parameters m_{rr} and mean RSI power = $k_2\pi_{rr}$, where k_2 ($0 \leq k_2 \leq 1$) represents the extent of SI cancellation; $k_2 = 0$ means RSI is absent in the system.

In the considered CDRT system, BS generates the NOMA signal by superposition coding and transmits $x(t)$ as

$$x(t) = \sqrt{P_s a_1} x_1(t) + \sqrt{P_s a_2} x_2(t) \quad (3)$$

where $x_1(t)$ and $x_2(t)$ are the information symbols for U_1 and U_2 respectively; a_1 and a_2 are the power allocation coefficients such that $a_1 + a_2 = 1$, $a_1 < a_2$; and P_s is the source power. Thus, the far user is allocated higher power as compared to the near user. According to the NOMA protocol employed, both R and U_1 will receive the NOMA signal. Now R will try to recover the symbol x_2 by treating signal corresponding to U_1 as interference. Under DF relaying, R will forward a clean copy of the re-encoded symbol x_2 to U_2 . Since it operates in the FD node, there will be RSI present at the receiver of R. Accordingly the received signal at R is

$$y_r(t) = \sqrt{P_s a_1} h_{sr} x_1(t) + \sqrt{P_s a_2} h_{sr} x_2(t) + \sqrt{P_r} h_{rr} x_2(t-\tau) + n_r(t) \quad (4)$$

In (4), the third term represents the RSI present at the relay node, P_r is the transmit power of R, τ is the processing delay, and $n_r(t)$ is the AWGN component at R. The relay tries to decode x_2 in the presence of signal corresponding to x_1 and RSI. The corresponding SINR is given by:

$$\Gamma_{r2} = \frac{|h_{sr}|^2 \rho_s a_2}{|h_{sr}|^2 \rho_s a_1 + |h_{rr}|^2 \rho_r + 1} \quad (5)$$

where $\rho_s = \frac{P_s}{\sigma^2}$ and $\rho_r = \frac{P_r}{\sigma^2}$. The corresponding achievable rate is given by:

$$C_{r2} = \log_2(1 + \Gamma_{r2}) \quad (6)$$

Once R forwards the re-encoded symbol x_2 , the received signal at U_2 is given by:

$$y_2(t) = h_{r2}x_2(t - \tau) + n_2(t) \quad (7)$$

where $n_2(t)$ is the AWGN component at U_2 . From the received signal, U_2 tries to recover the symbol x_2 and the corresponding SNR is

$$\Gamma_{22} = \rho_r |h_{r2}|^2 \quad (8)$$

The achievable rate for R- U_2 link is

$$C_{22} = \log_2(1 + \Gamma_{22}) \quad (9)$$

Meanwhile, the received signal at U_1 is given by

$$y_1(t) = \sqrt{P_s a_1} h_{s1} x_1(t) + \sqrt{P_s a_2} h_{s1} x_2(t) + \sqrt{P_r} h_{r1} x_2(t - \tau) + n_1(t) \quad (10)$$

Here, the third term represents the interference at U_1 arising due to transmissions from R. According to the NOMA principle, U_1 can decode the far user's symbol x_2 ; thus, $x_2(t - \tau)$ is known at U_1 apriori. Thus, U_1 can cancel the third term in (10) completely. However, we assume that perfect cancelation of the third term is not possible at U_1 ; thus, (10) is written as follows:

$$y_1(t) = \sqrt{P_s a_1} h_{s1} x_1(t) + \sqrt{P_s a_2} h_{s1} x_2(t) + \sqrt{P_r} \hat{h}_{r1} x_2(t - \tau) + n_1(t) \quad (11)$$

In (11), $|\hat{h}_{r1}|$ is assumed to have Nakgami PDF, and thus, $|\hat{h}_{r1}|^2$ has Gamma PDF with mean $k_1 \pi_{r1}$ where $k_1 (0 \leq k_1 \leq 1)$ represents the level of residual interference created at U_1 due to incomplete cancelation of interference from R. The SINR corresponding to the decoding of x_2 at U_1 is

$$\Gamma_{12} = \frac{|h_{s1}|^2 \rho_s a_2}{|h_{s1}|^2 \rho_s a_1 + |\hat{h}_{r1}|^2 \rho_r + 1} \quad (12)$$

The corresponding achievable rate is given by

$$C_{12} = \log_2(1 + \Gamma_{12}) \quad (13)$$

After decoding x_2 successfully, U_1 will decode x_1 by performing SIC. In this case, the decoded symbol x_2 must be subtracted from $y_1(t)$ before the decoding of x_1 is carried

out. If x_2 is decoded successfully, it can be completely subtracted from the composite received signal, i.e., SIC will be perfect. Otherwise, the decoding of x_1 will be carried out in the presence of residual interference due to I-SIC. Thus, SINR corresponding to the decoding of x_1 at U_1 in the presence of I-SIC is given by

$$\Gamma_{11} = \frac{|h_{s1}|^2 \rho_s a_1}{|h_{s1}|^2 \rho_s \beta a_2 + |\hat{h}_{r1}|^2 \rho_r + 1} \quad (14)$$

where $0 \leq \beta < 1$; i.e., $\beta = 0$ means P-SIC and $0 < \beta \leq 1$ implies I-SIC.

The achievable rate corresponding to the decoding of x_1 at U_1 is given by

$$C_{11} = \log_2(1 + \Gamma_{11}) \quad (15)$$

Under DF relaying, the maximum achievable rate for U_2 is given by

$$C_2 = \log_2[1 + \min(\Gamma_{12}, \Gamma_{r2}, \Gamma_{22})] \quad (16)$$

4 Performance analysis

In this section, we present analytical models for finding the outage probabilities and ergodic rates of U_1 and U_2 in the considered FDR-based NOMA-CDRT system. We derive closed form expressions for the system outage probability as well, under imperfect SIC condition.

4.1 Outage probability analysis

Assume that R_1 and R_2 (expressed in bits per channel use, i.e., bpcu) are the target rates for the successful decoding of symbols x_1 and x_2 , respectively, in the considered FDR-based NOMA-CDRT system. Let $u_1^{FD} = 2^{R_1} - 1$ and $u_2^{FD} = 2^{R_2} - 1$ be the corresponding SINR threshold values. If HDR technique is considered instead of FDR technique, the system requires two distinct time slots to complete the transmission of symbols x_1 and x_2 . Thus, achievable rate for HD system is halved. For a fair comparison, we set the target rates for the equivalent HDR-based NOMA-CDRT system to be the same as that of the FDR-based system. Accordingly, the SINR threshold values are given by $u_1^{HD} = 2^{2R_1} - 1$ and $u_2^{HD} = 2^{2R_2} - 1$ for U_1 and U_2 , respectively.

4.1.1 Outage probability experienced by U_1 in FDR-based NOMA-CDRT system

Notice that the near user U_1 would not experience outage if both x_1 and x_2 are decoded successfully at U_1 . Thus, the outage probability of U_1 is given by

$$P_{out,1}^{FD} = 1 - Pr\{\Gamma_{12} \geq u_2^{FD}; \Gamma_{11} \geq u_1^{FD}\} \quad (17)$$

Proposition 1: Assuming $u_2^{FD} < \frac{a_2}{a_1}$ and $u_1^{FD} < \frac{a_1}{\beta a_2}$, $P_{out,1}^{FD}$ is given by the following equation:

$$P_{out,1}^{FD} = 1 - \left[e^{-\frac{1}{\phi \rho_s \beta_{s1}}} \frac{(k_1 \beta_{r1})^{-m_{r1}}}{\Gamma(m_{r1})} \sum_{j=0}^{m_{s1}-1} \frac{1}{j!} \left(\frac{\rho_r}{\phi \rho_s \beta_{s1}} \right)^j \sum_{k=0}^j C_k \left(\frac{1}{\rho_r} \right)^{j-k} (m_{r1} + k - 1)! \times \left(\frac{\rho_r}{\phi \rho_s \beta_{s1}} + \frac{1}{\beta_{r1} k_1} \right)^{-m_{r1}-k} \right] \quad (18)$$

where $\phi = \min\left(\frac{a_2 - u_2^{FD} a_1}{u_2^{FD}}, \frac{a_1 - \beta a_2 u_1^{FD}}{u_1^{FD}}\right)$. Further, when either $u_2^{FD} \geq \frac{a_2}{a_1}$ or when $u_1^{FD} \geq \frac{a_1}{\beta a_2}$, $P_{out,1}^{FD}$ becomes unity. Proof: Refer Appendix A.

4.1.2 Outage probability experienced by U_2 in FDR-based NOMA-CDRT system

Notice that the far user U_2 would not suffer from outage if x_2 is decoded successfully at R and U_2 . Thus, the outage probability experienced by U_2 is given by

$$P_{out,2}^{FD} = 1 - Pr\{\Gamma_{r2} \geq u_2^{FD}, \Gamma_{22} \geq u_1^{FD}\} a \quad (19)$$

Proposition 2: Assuming that $u_2^{FD} < \frac{a_2}{a_1}$, $P_{out,2}^{FD}$ is given by the following expression

$$P_{out,2}^{FD} = 1 - \left[e^{-\frac{1}{\psi \rho_s \beta_{sr}}} \frac{(k_2 \beta_{rr})^{-m_{rr}}}{\Gamma(m_{rr})} \sum_{j=0}^{m_{sr}-1} \frac{1}{j!} \left(\frac{\rho_r}{\psi \rho_s \beta_{sr}} \right)^j \sum_{k=0}^j j C_k \left(\frac{1}{\rho_r} \right)^{j-k} (m_{rr} + k - 1)! \left(\frac{\rho_r}{\psi \rho_s \beta_{sr}} + \frac{1}{\beta_{rr} k_2} \right)^{-m_{rr}-k} e^{-\left(\frac{u_2^{FD}}{\rho_r \beta_{r2}}\right) m_{r2}-1} \sum_{i=0}^{m_{r2}-1} \frac{1}{i!} \left(\frac{u_2^{FD}}{\rho_r \beta_{r2}} \right)^i \right] \quad (20)$$

where $\psi = \frac{a_2 - u_2^{FD} a_1}{u_2^{FD}}$ and $j C_k = \frac{j!}{k!(j-k)!}$. Further, when $u_2^{FD} \geq \frac{a_2}{a_1}$, $P_{out,2}^{FD}$ becomes unity. Proof: Refer Appendix B.

4.1.3 System outage probability derivation

System outage probability is the probability of the event that either one user or both the users in the considered FDR-based NOMA-CDRT network suffer outage conditions. Thus, we determine the system outage probability as follows:

$$P_{out,sys}^{FD} = 1 - Pr\{\Gamma_{12} \geq u_2^{FD}, \Gamma_{11} \geq u_1^{FD}, \Gamma_{r2} \geq u_2^{FD}, \Gamma_{22} \geq u_1^{FD}\} \quad (21a)$$

To find the closed form expression for the system outage probability, we substitute the expressions for Γ_{12} , Γ_{11} , Γ_{r2} , and Γ_{22} in (21a). Accordingly, $P_{out,sys}^{FD}$ becomes:

$$P_{out,sys}^{FD} = 1 - Pr\left\{ \frac{|h_{s1}|^2 \rho_s a_2}{|h_{s1}|^2 \rho_s a_1 + |\hat{h}_{r1}|^2 \rho_r + 1} \geq u_2^{FD}, \frac{|h_{s1}|^2 \rho_s a_1}{|\hat{h}_{r1}|^2 \rho_r + 1} \geq u_1^{FD}, \right. \quad (21b)$$

$$\left. \frac{|h_{sr}|^2 \rho_s a_2}{|h_{sr}|^2 \rho_s a_1 + |h_{r2}|^2 \rho_r + 1} \geq u_2^{FD}, \rho_r |h_{r2}|^2 \geq u_2^{FD} \right\} = 1 - Pr\left\{ |h_{s1}|^2 \rho_s \geq \frac{u_2^{FD} (|\hat{h}_{r1}|^2 \rho_r + 1)}{(a_2 - u_2^{FD} a_1)}; |h_{s1}|^2 \rho_s \geq \frac{u_1^{FD} (|\hat{h}_{r1}|^2 \rho_r + 1)}{(a_1 - u_1^{FD} a_1 \beta)}; \right. \quad (21c)$$

$$\left. |h_{sr}|^2 \rho_s \geq \frac{u_2^{FD} (|h_{r2}|^2 \rho_r + 1)}{(a_2 - u_2^{FD} a_1)}; |h_{r2}|^2 \rho_r \geq u_2^{FD} \right\} = 1 - Pr\left\{ |h_{s1}|^2 \rho_s \geq \frac{1}{\phi} (|\hat{h}_{r1}|^2 \rho_r + 1); |h_{sr}|^2 \rho_s \geq \frac{(|h_{r2}|^2 \rho_r + 1)}{\psi}; |h_{r2}|^2 \rho_r \geq u_2^{FD} \right\} \quad (21d)$$

In (21d), the constants ϕ and ψ were defined in propositions 1 and 2, respectively. Now, the channel power gains, $|h_{sr}|^2$, $|h_{s1}|^2$, and $|h_{r2}|^2$ are independent since they correspond to distinct communication links in the network. Thus, $P_{out,sys}^{FD}$ is given by

$$P_{out,sys}^{FD} = 1 - \left[Pr\left\{ |h_{s1}|^2 \rho_s \geq \frac{1}{\phi} (|\hat{h}_{r1}|^2 \rho_r + 1) \right\} \times Pr\left\{ |h_{sr}|^2 \rho_s \geq \frac{(|h_{r2}|^2 \rho_r + 1)}{\psi} \right\} \times Pr\left\{ |h_{r2}|^2 \rho_r \geq u_2^{FD} \right\} \right] \quad (21e)$$

Proposition 3: Assuming that $u_2^{FD} < \frac{a_2}{a_1}$ and $u_1^{FD} < \frac{a_1}{\beta a_2}$, the closed form expression for $P_{out,sys}^{FD}$ is given as follows:

$$\begin{aligned}
P_{out,sys}^{FD} &= 1 - \left[e^{-\frac{1}{\phi\rho_s\beta_{s1}}(k_1\beta_{r1})^{-m_{r1}}} \frac{\Gamma(m_{r1})}{\Gamma(m_{r1})} \right. \\
&\quad \sum_{j=0}^{m_{s1}-1} \frac{1}{j!} \left(\frac{\rho_r}{\phi\rho_s\beta_{s1}} \right)^j \sum_{k=0}^j {}^j C_k \left(\frac{1}{\rho_r} \right)^{j-k} \\
&\quad (m_{r1} + k - 1)! \times \left(\frac{\rho_r}{\phi\rho_s\beta_{s1}} + \frac{1}{\beta_{r1}k_1} \right)^{-m_{r1}-k} \\
&\quad \times e^{-\frac{1}{\psi\rho_s\beta_{sr}}(k_2\beta_{rr})^{-m_{rr}}} \\
&\quad \sum_{l=0}^{m_{sr}-1} \frac{1}{l!} \left(\frac{\rho_r}{\psi\rho_s\beta_{sr}} \right)^l \sum_{q=0}^l {}^l C_q \left(\frac{1}{\rho_r} \right)^{l-q} (m_{rr} + q - 1)! \\
&\quad \left(\frac{\rho_r}{\psi\rho_s\beta_{sr}} + \frac{1}{\beta_{rr}k_2} \right)^{-m_{rr}-q} e^{-\left(\frac{u_2^{FD}}{\rho_r\beta_{r2}}\right)} \\
&\quad \left. \sum_{i=0}^{m_{r2}-1} \frac{1}{i!} \left(\frac{u_2^{FD}}{\rho_r\beta_{r2}} \right)^i \right] \quad (21f)
\end{aligned}$$

When either $u_2^{FD} \geq \frac{a_2}{a_1}$ or $u_1^{FD} \geq \frac{a_1}{\beta a_2}$, $P_{out,sys}^{FD}$ becomes unity.

Proof: Appendix C.

4.2 Ergodic rate analysis

In this section, we analyze the ergodic rates achieved by U_1 and U_2 in the presence of I-SIC condition.

4.2.1 Ergodic rate from BS to U_1 in FDR-based NOMA-CDRT system

The ergodic rate achieved by the near user U_1 ($E[R_1^{FD}]$) is determined as follows:

$$\begin{aligned}
E[R_1^{FD}] &= \mathbb{E}[\log_2(1 + \Gamma_{11})] \\
&= \int_0^\infty \log_2(1 + x) f_{\Gamma_{11}}(x) dx \\
&= \frac{1}{\ln 2} \int_0^\infty \frac{1 - F_{\Gamma_{11}}(x)}{1 + x} dx \quad (22a)
\end{aligned}$$

where $F_{\Gamma_{11}}(x)$ and $f_{\Gamma_{11}}(x)$ are the CDF and PDF of Γ_{11} , respectively.

Proposition 4: An approximate closed form expression for $E[R_1^{FD}]$ is given as follows.

$$\begin{aligned}
E[R_1^{FD}] &\cong \frac{1}{\ln 2} \frac{(k_1\beta_{r1})^{-m_{r1}}}{\Gamma(m_{r1})} \sum_{j=0}^{m_{s1}-1} \frac{1}{j!} \sum_{k=0}^j {}^j C_k \left(\frac{1}{\rho_r} \right)^{j-k} \\
&\quad (m_{r1} + k - 1)! \times \frac{\pi}{N} \sum_{n=0}^N \frac{a_n b_n}{d_n} e^{-c_n} \quad (22b)
\end{aligned}$$

where $a_n = \left(\frac{a_1\rho_r(1+\phi_n)}{\beta a_2\rho_s a_1(1-\phi_n)} \right)^j \sqrt{1-\phi_n^2}$, $b_n = \left(\frac{a_1\rho_r(1+\phi_n)}{\beta a_2\rho_s a_1(1-\phi_n)} + \frac{1}{k_1\beta_{r1}} \right)^{m_{r1}-k}$, $c_n = \frac{a_1(1+\phi)}{\beta a_2\rho_s a_1(1-\phi_n)}$, $d_n = \frac{2\beta a_2 + a_1(1+\phi_n)}{2\beta a_2}$ and $\phi_n = \cos\left(\frac{(2n-1)\pi}{2N}\right)$. Notice

that (22b) is obtained by using the Gaussian-Chebyshev quadrature formula, which is described in Appendix D. Here, N is the complexity accuracy trade-off parameter in this approximation.

Proof: Refer Appendix D.

4.2.2 Ergodic rate from BS to U_2 in FDR-based NOMA-CDRT system

The ergodic rate achieved by the far user U_2 ($E[R_2^{FD}]$) is determined as follows:

$$\begin{aligned}
E[R_2^{FD}] &= \mathbb{E}[\log_2(1 + \min\{\Gamma_{12}, \Gamma_{r2}, \Gamma_{22}\})] \\
&= \mathbb{E}[\log_2(1 + Y)] \\
&= \frac{1}{\ln 2} \int_0^\infty \frac{1 - F_Y(y)}{1 + y} dy \quad (23a)
\end{aligned}$$

where $y = \min\{\Gamma_{12}, \Gamma_{r2}, \Gamma_{22}\}$ and $F_Y(y)$ is the CDF of Y .

Proposition 5: An approximate closed form expression for $E[R_2^{FD}]$ is given as follows.

$$\begin{aligned}
E[R_2^{FD}] &\cong \frac{(k_1\beta_{r1})^{-m_{r1}}}{\Gamma(m_{r1})} \sum_{j=0}^{m_{s1}-1} \frac{1}{j!} \sum_{k=0}^j {}^j C_k \left(\frac{1}{\rho_r} \right)^{j-k} \\
&\quad \times (m_{r1} + k - 1)! \frac{(k_2\beta_{rr})^{-m_{rr}}}{\Gamma(m_{rr})} \\
&\quad \times \sum_{l=0}^{m_{sr}-1} \frac{1}{l!} \sum_{p=0}^l {}^l C_p \left(\frac{1}{\rho_r} \right)^{l-p} (m_{rr} + p - 1)! \\
&\quad \times \sum_{q=0}^{m_{r2}-1} \frac{1}{q!} \times \frac{\pi}{N \ln 2} \\
&\quad \times \sum_{n=0}^N \frac{e_n f_n g_n h_n r_n}{w_n} e^{-s_n} e^{-t_n} e^{-v_n} \quad (23b)
\end{aligned}$$

where $e_n = \left(\frac{(1+\phi_n)}{a_1\rho_s(1-\phi_n)\beta_{s1}} + \frac{1}{\beta_{r1}k_1} \right)^{-m_{r1}-k} \sqrt{1-\phi_n^2}$, $f_n = \left(\frac{(1+\phi_n)}{a_1\rho_s(1-\phi_n)\beta_{s1}} \right)^j$, $g_n = \left(\frac{(1+\phi_n)}{a_1\rho_s(1-\phi_n)\beta_{sr}} \right)^l$, $h_n = \left(\frac{(1+\phi_n)}{a_1\rho_s(1-\phi_n)\beta_{s1}} + \frac{1}{\beta_{rr}k_2} \right)^{-m_{rr}-p}$, $r_n = \left(\frac{a_2(1+\phi_n)}{2a_1\rho_r\beta_{r2}} \right)^q$, $s_n = \frac{2a_1+a_2(1+\phi_n)}{2a_1\rho_r\beta_{r2}}$, $t_n = \frac{(1+\phi_n)}{a_1\rho_s(1-\phi_n)\beta_{s1}}$, $v_n = \frac{(1+\phi_n)}{a_1\rho_s(1-\phi_n)\beta_{sr}}$, $w_n = \frac{a_2(1+\phi_n)}{2a_1\rho_r\beta_{r2}}$, $\phi_n = \cos\left(\frac{(2n-1)\pi}{2N}\right)$ and N is the complexity accuracy trade-off parameter, relating to the Gaussian-Chebyshev quadrature method.

Proof: Appendix E.

5 Optimal power allocation (OPA) for minimizing system outage probability

In this section, our aim is to find the OPA factor at the BS, i.e., $a_{1,opt}$ that minimizes the system outage probability in

FDR-based NOMA-CDRT system. The outage minimization problem can be formulated as

$$\begin{aligned} \min_{a_1} \quad & P_{out,sys}^{FD} \\ \text{s.t.} \quad & a_1 + a_2 = 1 \end{aligned} \quad (24)$$

Proposition 5: For the considered FDR-based NOMA-CDRT system, the OPA coefficient $a_{1,opt}$ that minimizes the system outage probability is given by

$$a_{1,opt} = \frac{u_1^{FD}}{u_1^{FD} + u_2^{FD} + u_1^{FD}u_2^{FD}} \quad (25)$$

Proof:

Recall the expression for the system outage probability given in section 4, i.e.,

$$P_{out,sys}^{FD} = 1 - (C_0 \times A_0 \times B_0) \quad (26)$$

Here, A_0 and B_0 are given by (42) and (43), respectively, and $C_0 = 1 - P_{out,1}^{FD}$, where $P_{out,1}^{FD}$ is given by (18). These are reproduced below:

$$\begin{aligned} A_0 = e^{-\frac{1}{\psi\rho_s\beta_{sr}}} \frac{(k_2\beta_{rr})^{-m_{rr}}}{\Gamma(m_{rr})} \sum_{l=0}^{m_{sr}-1} \frac{1}{l!} \left(\frac{\rho_r}{\psi\rho_s\beta_{sr}} \right)^l \\ \times \sum_{q=0}^l {}^l C_q \left(\frac{1}{\rho_r} \right)^{l-q} (m_{rr} + q - 1)! \\ \times \left(\frac{\rho_r}{\psi\rho_s\beta_{sr}} + \frac{1}{\beta_{rr}k_2} \right)^{-m_{rr}-q} \end{aligned} \quad (27)$$

$$\begin{aligned} B_0 = Pr\{|h_{r2}|^2 \rho_r \geq u_2^{FD}\} = Pr\{|h_{r2}|^2 \geq \frac{u_2^{FD}}{\rho_r}\} \\ = e^{-\left(\frac{u_2^{FD}}{\rho_r\beta_{r2}}\right)} \sum_{i=0}^{m_{r2}-1} \frac{1}{i!} \left(\frac{u_2^{FD}}{\rho_r\beta_{r2}} \right)^i \end{aligned} \quad (28)$$

$$\begin{aligned} C_0 = e^{-\frac{1}{\phi\rho_s\beta_{s1}}} \frac{(k_1\beta_{r1})^{-m_{r1}}}{\Gamma(m_{r1})} \sum_{j=0}^{m_{s1}-1} \frac{1}{j!} \left(\frac{\rho_r}{\phi\rho_s\beta_{s1}} \right)^j \\ \times \sum_{k=0}^j {}^j C_k \left(\frac{1}{\rho_r} \right)^{j-k} \\ (m_{r1} + k - 1)! \times \left(\frac{\rho_r}{\phi\rho_s\beta_{s1}} + \frac{1}{\beta_{r1}k_1} \right)^{-m_{r1}-k} \end{aligned} \quad (29)$$

It is assumed that SIC is perfect, i.e., $\beta = 0$ in this section. Notice that in the expression for A_0 , ψ must be greater than 0 which implies $u_2^{FD} < \frac{a_2}{a_1}$. Since $a_2 = 1 - a_1$, this implies that a_1 must satisfy the condition $0 < a_1 < \frac{1}{1+u_2^{FD}}$. Now,

consider $C_0 = 1 - P_{out,1}^{FD}$ where $\phi = \min\left(\frac{a_2 - u_2^{FD}a_1}{u_2^{FD}}, \frac{a_1}{u_1^{FD}}\right)$, which will give rise to two distinct cases as given below:

$$\text{Case(I): } \frac{a_2 - u_2^{FD}a_1}{u_2^{FD}} < \frac{a_1}{u_1^{FD}}$$

Since $a_2 = 1 - a_1$, the above implies that a_1 must satisfy the following condition: $\frac{u_1^{FD}}{u_1^{FD} + u_2^{FD} + u_1^{FD}u_2^{FD}} < a_1 < \frac{1}{1+u_2^{FD}}$. In this case, the system outage can be written as follows:

$$P_{out,sys}^{FD} = 1 - (A_0(a_1) \times B_0 \times C_0(a_1)) \quad (30)$$

where $A_0(a_1)$ and $C_0(a_1)$ are given by

$$\begin{aligned} A_0(a_1) = e^{-\frac{1}{(1-a_1-a_1u_2^{FD})\rho_s\beta_{sr}}} \frac{(k_2\beta_{rr})^{-m_{rr}}}{\Gamma(m_{rr})} \sum_{l=0}^{m_{sr}-1} \\ \frac{1}{l!} \left(\frac{u_2^{FD}\rho_r}{(1-a_1-a_1u_2^{FD})\rho_s\beta_{sr}} \right)^l \\ \times \sum_{q=0}^l {}^l C_q \left(\frac{1}{\rho_r} \right)^{l-q} (m_{rr} + q - 1)! \\ \left(\frac{u_2^{FD}\rho_r}{(1-a_1-a_1u_2^{FD})\rho_s\beta_{sr}} + \frac{1}{k_2\beta_{rr}} \right)^{-m_{rr}-q} \end{aligned} \quad (31a)$$

$$\begin{aligned} C_0(a_1) = e^{-\frac{u_2^{FD}}{(1-a_1-a_1u_2^{FD})\rho_s\beta_{s1}}} \frac{(k_1\beta_{r1})^{-m_{r1}}}{\Gamma(m_{r1})} \sum_{j=0}^{m_{s1}-1} \\ \frac{1}{j!} \left(\frac{u_2^{FD}\rho_r}{(1-a_1-a_1u_2^{FD})\rho_s\beta_{s1}} \right)^j \\ \times \sum_{k=0}^j {}^j C_k \left(\frac{1}{\rho_r} \right)^{j-k} (m_{r1} + k - 1)! \\ \left(\frac{u_2^{FD}\rho_r}{(1-a_1-a_1u_2^{FD})\rho_s\beta_{s1}} + \frac{1}{k_1\beta_{r1}} \right)^{-m_{r1}-k} \end{aligned} \quad (31b)$$

Notice that (31a) and (31b) are obtained by substituting $\psi = \phi = \frac{1-a_1-u_2^{FD}a_1}{u_2^{FD}}$ in (42) and (18), respectively. The derivative of $P_{out,sys}^{FD}(a_1)$ with respect to a_1 can be written as

$$[P_{out,sys}^{FD}(a_1)]' = -B_0[A_0(a_1)C_0'(a_1) + A_0'(a_1)C_0(a_1)] \quad (32)$$

where the first derivatives $A_0'(a_1)$ and $C_0'(a_1)$ can be determined by differentiating (31a) and (31b), respectively, with respect to a_1 . Thus, we write $A_0'(a_1) \triangleq x(a_1) + y(a_1) + z(a_1)$ where $x(a_1)$, $y(a_1)$ and $z(a_1)$ are given as follows:

$$x(a_1) = \frac{-\frac{u_2^{FD}}{\rho_s \beta_{sr}}(u_2^{FD} + 1)e^{-\frac{u_2^{FD}}{(1-a_1-a_1 u_2^{FD})\rho_s \beta_{sr}}}}{(1-a_1-a_1 u_2^{FD})^2} \frac{(k_2 \beta_{rr})^{-m_{rr}}}{\Gamma(m_{rr})}$$

$$\times \sum_{q=0}^l C_q^l \left(\frac{1}{\rho_r}\right)^l \left(\frac{u_2^{FD} \rho_r}{(1-a_1-a_1 u_2^{FD})\rho_s \beta_{sr}}\right)^l$$

$$\left(\frac{u_2^{FD} \rho_r}{(1-a_1-a_1 u_2^{FD})\rho_s \beta_{sr}} + \frac{1}{k_2 \beta_{rr}}\right)^{-m_{rr}-q} \quad (33a)$$

$$y(a_1) = e^{-\frac{u_2^{FD}}{(1-a_1-a_1 u_2^{FD})\rho_s \beta_{sr}}} \frac{(k_2 \beta_{rr})^{-m_{rr}}}{\Gamma(m_{rr})}$$

$$\sum_{l=0}^{m_{sr}-1} \frac{1}{l!} \frac{-\frac{u_2^{FD} \rho_r}{\rho_s \beta_{s1}} l(-u_2^{FD} - 1) \left(\frac{u_2^{FD} \rho_r}{\rho_s \beta_{s1}(1-a_1-a_1 u_2^{FD})}\right)^{l-1}}{(1-a_1-a_1 u_2^{FD})^2}$$

$$\times \sum_{q=0}^l C_q^l \left(\frac{1}{\rho_r}\right)^{l-q} (m_{rr} + q - 1)!$$

$$\left(\frac{u_2^{FD} \rho_r}{(1-a_1-a_1 u_2^{FD})\rho_s \beta_{sr}} + \frac{1}{k_2 \beta_{rr}}\right)^{-m_{rr}-q} \quad (33b)$$

$$z(a_1) = e^{-\frac{u_2^{FD}}{(1-a_1-a_1 u_2^{FD})\rho_s \beta_{sr}}} \frac{(k_2 \beta_{rr})^{-m_{rr}}}{\Gamma(m_{rr})}$$

$$\sum_{l=0}^{m_{sr}-1} \frac{1}{l!} \left(\frac{u_2^{FD} \rho_r}{(1-a_1-a_1 u_2^{FD})\rho_s \beta_{sr}}\right)^l$$

$$\times \sum_{q=0}^l C_q^l \left(\frac{1}{\rho_r}\right)^{l-q} (m_{rr} + q - 1)!$$

$$\frac{\frac{u_2 \rho_r}{\rho_s \beta_{s1}} (m_{rr} + q)(-u_2^{FD} - 1)}{(1-a_1-a_1 u_2^{FD})^2}$$

$$\times \left(\frac{u_2^{FD} \rho_r}{(1-a_1-a_1 u_2^{FD})\rho_s \beta_{sr}} + \frac{1}{k_2 \beta_{rr}}\right)^{-m_{rr}-q-1} \quad (33c)$$

In a similar way, we write $C'_0(a_1) = f(a_1) + g(a_1) + h(a_1)$ where $f(a_1)$, $g(a_1)$ and $h(a_1)$ are given as follows:

$$f(a_1) = \frac{-\frac{u_2^{FD}}{\rho_s \beta_{s1}}(u_2^{FD} + 1)e^{-\frac{u_2^{FD}}{(1-a_1-a_1 u_2^{FD})\rho_s \beta_{s1}}}}{(1-a_1-a_1 u_2^{FD})^2} \frac{(k_2 \beta_{r1})^{-m_{r1}}}{\Gamma(m_{r1})}$$

$$\times \sum_{j=0}^{m_{s1}-1} \frac{1}{j!} \left(\frac{u_2^{FD} \rho_r}{(1-a_1-a_1 u_2^{FD})\rho_s \beta_{s1}}\right)^j$$

$$\times \sum_{k=0}^j C_k^j \left(\frac{1}{\rho_r}\right)^{j-k} (m_{r1} + k - 1)!$$

$$\times \left(\frac{u_2^{FD} \rho_r}{(1-a_1-a_1 u_2^{FD})\rho_s \beta_{s1}} + \frac{1}{k_2 \beta_{r1}}\right)^{-m_{r1}-k} \quad (34a)$$

$$g(a_1) = e^{-\frac{u_2^{FD}}{(1-a_1-a_1 u_2^{FD})\rho_s \beta_{s1}}} \frac{(k_2 \beta_{r1})^{-m_{r1}}}{\Gamma(m_{r1})}$$

$$\times \sum_{j=0}^{m_{s1}-1} \frac{1}{j!} \frac{-\frac{u_2^{FD} \rho_r}{\rho_s \beta_{s1}} j(-u_2^{FD} - 1) \left(\frac{u_2^{FD} \rho_r}{\rho_s \beta_{s1}(1-a_1-a_1 u_2^{FD})}\right)^{j-1}}{(1-a_1-a_1 u_2^{FD})^2}$$

$$\times \sum_{k=0}^j C_k^j \left(\frac{1}{\rho_r}\right)^{j-k} (m_{r1} + k - 1)!$$

$$\times \left(\frac{u_2^{FD} \rho_r}{(1-a_1-a_1 u_2^{FD})\rho_s \beta_{s1}} + \frac{1}{k_2 \beta_{r1}}\right)^{-m_{r1}-k} \quad (34b)$$

$$h(a_1) = e^{-\frac{u_2^{FD}}{(1-a_1-a_1 u_2^{FD})\rho_s \beta_{s1}}} \frac{(k_2 \beta_{r1})^{-m_{r1}}}{\Gamma(m_{r1})}$$

$$\times \sum_{j=0}^{m_{s1}-1} \frac{1}{j!} \left(\frac{u_2^{FD} \rho_r}{(1-a_1-a_1 u_2^{FD})\rho_s \beta_{s1}}\right)^j$$

$$\times \sum_{k=0}^j C_k^j \left(\frac{1}{\rho_r}\right)^{j-k} (m_{r1} + k - 1)!$$

$$\times \frac{\frac{u_2 \rho_r}{\rho_s \beta_{s1}} (m_{r1} + k)(-u_2^{FD} - 1)}{(1-a_1-a_1 u_2^{FD})^2}$$

$$\times \left(\frac{u_2^{FD} \rho_r}{(1-a_1-a_1 u_2^{FD})\rho_s \beta_{s1}} + \frac{1}{k_2 \beta_{r1}}\right)^{-m_{r1}-k-1} \quad (34c)$$

Through numerical investigations, we observe that $[P_{out,sys}^{FD}]' > 0$, for the range of a_1 considered. Thus, we conclude that $P_{out,sys}^{FD}$ is a monotonically increasing function of a_1 for $\frac{u_1^{FD}}{u_1^{FD} + u_2^{FD} + u_1^{FD} u_2^{FD}} < a_1 < \frac{1}{1+u_2^{FD}}$.

Case II: $\frac{a_2 - u_2^{FD} a_1}{u_2^{FD}} > \frac{a_1}{u_1^{FD}}$

Since $a_2 = 1 - a_1$, the above condition implies that a_1 must satisfy $0 < a_1 < \frac{u_1^{FD}}{u_1^{FD} + u_2^{FD} + u_1^{FD} u_2^{FD}}$. In this case, the system outage probability can be written as $P_{out,sys}^{FD}(a_1) = 1 - [A_0(a_1) \times B_0 \times C_1(a_1)]$ where $A_0(a_1)$ is given by (31a) and $C_1(a_1)$ is obtained by substituting $\phi = \frac{a_1}{u_1^{FD}}$ in the expression for $C_0 = 1 - P_{out,1}^{FD}$, with $P_{out,1}^{FD}$ given by (18). Thus, $C_1(a_1)$ is given by

$$C_1(a_1) = e^{-\frac{u_1^{FD}}{a_1 \rho_s \beta_{s1}}} \frac{(k_1 \beta_{r1})^{-m_{r1}}}{\Gamma(m_{r1})} \sum_{j=0}^{m_{sr}-1} \frac{1}{j!} \left(\frac{u_1^{FD} \rho_r}{a_1 \rho_s \beta_{s1}}\right)^j$$

$$\times \sum_{k=0}^j C_k^j \left(\frac{1}{\rho_r}\right)^{j-k} (m_{r1} + k - 1)!$$

$$\times \left(\frac{u_1^{FD} \rho_r}{a_1 \rho_s \beta_{s1}} + \frac{1}{k_1 \beta_{r1}}\right)^{-m_{r1}-k} \quad (35)$$

The first-order derivative of $P_{out,sys}^{FD}$ is computed as $[P_{out,sys}^{FD}(a_1)]' = -B_0[A_0(a_1)C_1'(a_1) + A_0'(a_1)C_1(a_1)]$. Notice that $A_0'(a_1)$, which is the first order derivative of $A_0(a_1)$, can be determined by combining (33a)-(33c) as in the previous case I. The first derivative of $C_1(a_1)$, i.e., $C_1'(a_1)$ is given by $C_1'(a_1) = u(a_1) + v(a_1) + w(a_1)$ where $u(a_1)$, $v(a_1)$, and $w(a_1)$ are given by

$$u(a_1) = \frac{-\frac{u_1^{FD}}{\rho_s \beta_{s1}} e^{-\frac{u_1^{FD}}{a_1 \rho_s \beta_{s1}}}}{a_1^2} \frac{(k_1 \beta_{r1})^{-m_{r1}}}{\Gamma(m_{r1})} \sum_{j=0}^{m_{sr}-1} \times \frac{1}{j!} \left(\frac{u_1^{FD} \rho_r}{a_1 \rho_s \beta_{s1}} \right)^j \sum_{k=0}^j j C_k \left(\frac{1}{\rho_r} \right)^{j-k} \times (m_{r1} + k - 1)! \left(\frac{u_1^{FD} \rho_r}{a_1 \rho_s \beta_{s1}} + \frac{1}{k_1 \beta_{r1}} \right)^{-m_{r1}-k} \quad (36a)$$

$$v(a_1) = e^{-\frac{u_1^{FD}}{a_1 \rho_s \beta_{s1}}} \frac{(k_1 \beta_{r1})^{-m_{r1}}}{\Gamma(m_{r1})} \sum_{j=0}^{m_{sr}-1} \frac{1}{j!} \frac{-j \left(\frac{u_1^{FD} \rho_r}{a_1 \rho_s \beta_{s1}} \right)^j}{a_1} \times \sum_{k=0}^j j C_k \left(\frac{1}{\rho_r} \right)^{j-k} (m_{r1} + k - 1)! \times \left(\frac{u_1^{FD} \rho_r}{a_1 \rho_s \beta_{s1}} + \frac{1}{k_1 \beta_{r1}} \right)^{-m_{r1}-k} \quad (36b)$$

$$w(a_1) = e^{-\frac{u_1^{FD}}{a_1 \rho_s \beta_{s1}}} \frac{(k_1 \beta_{r1})^{-m_{r1}}}{\Gamma(m_{r1})} \sum_{j=0}^{m_{sr}-1} \frac{1}{j!} \left(\frac{u_1^{FD} \rho_r}{a_1 \rho_s \beta_{s1}} \right)^j \times \sum_{k=0}^j j C_k \left(\frac{1}{\rho_r} \right)^{j-k} (m_{r1} + k - 1)! \times \frac{\frac{u_1^{FD} \rho_r}{\rho_s \beta_{s1}} (m_{r1} + k) \left(\frac{u_1^{FD} \rho_r}{a_1 \rho_s \beta_{s1}} + \frac{1}{k_1 \beta_{r1}} \right)^{-m_{r1}-k-1}}{a_1^2} \quad (36c)$$

Through numerical investigations, we find that the first derivative $[P_{out,sys}^{FD}]' < 0$ for the range of a_1 considered. Hence, we conclude that $P_{out,sys}^{FD}$ is a decreasing function of a_1 if $0 < a_1 < \frac{u_1^{FD}}{u_1^{FD} + u_2^{FD} + u_1^{FD} u_2^{FD}}$.

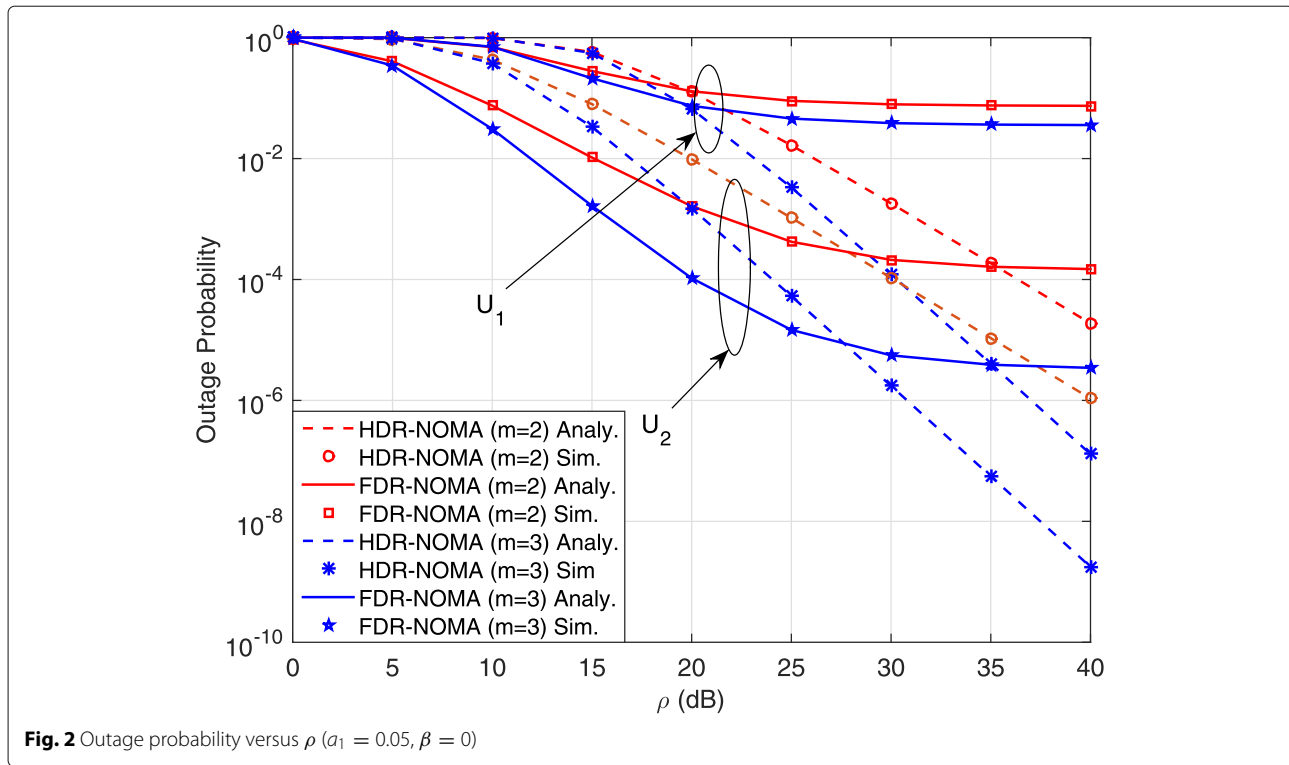
Thus, we observe that $P_{out,sys}^{FD}$ is a monotonically decreasing function of a_1 for $0 < a_1 < \frac{u_1^{FD}}{u_1^{FD} + u_2^{FD} + u_1^{FD} u_2^{FD}}$ and monotonically increasing function of a_1 for $\frac{u_1^{FD}}{u_1^{FD} + u_2^{FD} + u_1^{FD} u_2^{FD}} < a_1 < \frac{1}{1 + u_2^{FD}}$. Thus, the optimal value of the power allocation coefficient a_1 that minimizes the

system outage is obtained as $a_{1,opt} = \frac{u_1^{FD}}{u_1^{FD} + u_2^{FD} + u_1^{FD} u_2^{FD}}$. This completes the proof.

6 Performance evaluation results and discussion

This section describes the results for the outage and the ergodic rate performance of the two users in the considered CDRT system. The analytical results are validated by performing extensive Monte Carlo simulations considering a set of 10^5 channel realizations. We select $\rho_s = \rho_r = \rho$, $m_{ij} = m$, where ρ is directly related to the transmit power. Unless otherwise specified, the following parameters are chosen for the evaluation: $R_1 = 1$ bpcu, $R_2 = 1$ bpcu, $m = 2$, and $n = 3$. We consider a two dimensional topology for the network under consideration with (x_i, y_i) representing the coordinates of a given node i . Assume that BS is placed at $(0,0)$ and BS, R, and U_2 are placed on a straight line. Let the coordinates of R and U_2 be $(1.25,0)$ and $(1.75,0)$, respectively. Further, we choose the coordinates of U_1 as $(0.625,0.5)$ so that the distances between these nodes are $d_{s1} = 0.8d_0$, $d_{sr} = 1.25d_0$, $d_{r1} = 0.8d_0$, $d_{r2} = 0.5d_0$. Here, d_0 is the reference distance and is selected as 1 km. For numerical illustrations, we set $k_1 = 10^{-2}$, $k_2 = 0.64 \times 10^{-2}$; however, the results can be modified for any given values of k_1 and k_2 ($0 \leq k_1, k_2 \leq 1$). Further, we choose $\pi_{ij} = E[|h_{ij}|^2] = \left(\frac{d_{ij}}{d_0}\right)^{-n}$, $i \in (s, r)$, $j \in (r, 1, 2)$ with π_{rr} set as equal to -3 dB. For comparison purpose, we consider HDR-based NOMA-CDRT system as well, where the communication is completed in two time slots. In the first time slot, BS transmits the NOMA signal consisting of symbols x_1 and x_2 . U_1 decodes x_1 by implementing SIC, while R decodes x_2 and forwards the symbol in the second time slot. Finally, x_2 is decoded successfully at U_2 . Here, we assume that U_1 would not receive interference from R's transmission since it happens in the second time slot during which U_1 is silent. We modify the relevant equations of Section 4 to find the outage of U_1 and U_2 in HDR-NOMA-CDRT system. For a fair comparison among FDR and HDR systems, we consider the target rate of HDR system to be the same as that of FDR system. Since HDR system requires additional time slots for completing the transmission of symbols, the achievable rate is reduced as compared to FDR system. For the outage calculation, since the target rate for both HDR-CDRT and FDR-CDRT systems are assumed to be equal, it leads to higher SINR threshold requirement for the users in HDR-NOMA-CDRT system, as compared to the equivalent FDR system.

In Fig. 2, the outage probabilities experienced by U_1 and U_2 are drawn against ρ for FDR/HDR-based NOMA-CDRT system. Results show that, as ρ increases, the outage performance of both the users is improved. Further, the results in Fig. 2 show that U_1 suffers higher outage probability than U_2 for a given set of parameters. This



happens because the power allocation factor at BS, i.e., a_1 has been chosen arbitrarily. In addition, the decoding of symbol x_1 at U_1 requires a two-step procedure: successful decoding of symbol x_2 by treating signal corresponding to x_1 as interference, which is followed by decoding of x_1 by applying SIC to cancel the known x_2 . In this process, U_1 is affected by interference due to transmissions from R as well. However, decoding of x_2 happens at U_2 in the absence of interference from any source. Moreover, it is assumed that the relay forwards the re-encoded version of x_2 with full power which increases the probability of successful decoding of x_2 at U_2 . As ρ is varied, the outage performance of U_1 and U_2 shows distinct behavior in FDR/HDR-NOMA-CDRT systems. In the low transmit power region, the outage probabilities experienced by both U_1 and U_2 in FDR-NOMA-CDRT system is lower as compared to the outage experienced in HDR-NOMA-CDRT system. This happens due to the higher threshold SINR requirement for HDR system as mentioned before. However, in the high transmit power region, the mean RSI power at R ($k_2\pi_{rr}$) becomes higher in FDR-based system, triggering degradation of SINR at R . This increases the outage of U_2 in FDR-NOMA-CDRT system in the high transmit power region, as compared to HDR system as can be seen in Fig. 2. At the same time, the outage performance of U_1 is not affected by the RSI at R in FDR-NOMA-CDRT system, as the decoding of x_2 or x_1 at U_1 is not affected by the SINR over BS- R link. However,

the decoding at U_1 is affected by the residual interference ($k_1\pi_{r1}$) created due to transmission over the R - U_2 link in FDR-NOMA-CDRT system, which becomes significantly higher when transmit power is increased. Thus, the outage experienced by U_1 in FDR-NOMA-CDRT system becomes significantly higher in the high transmit power region. Notice that this residual interference is absent in HDR system, and thus, U_1 exhibits much improved performance in HDR-NOMA-CDRT system when transmit power is increased.

Figure 3 shows the impact of I-SIC factor β on the outage probability performance of U_1 and U_2 in FDR-NOMA-CDRT system. As β increases, $P_{out,1}^{FD}$ increases owing to the higher amount of interference generated by I-SIC at U_1 . However, $P_{out,2}^{FD}$ is not influenced by β , since U_2 (being the far-user) does not implement SIC for decoding symbol x_2 . As β increases from 0.3 to 0.4, $P_{out,1}^{FD}$ increases by 89% for $\rho = 30$ dB.

Figure 4 shows the outage probability of U_1 in FDR-NOMA-CDRT system against the mean residual interference ($k_1\pi_{r1}$) present at U_1 (which is generated by the inaccurate cancelation of symbol x_2 at U_1). The results show that the mean residual interference has significant impact on the outage of U_1 . The results in Fig. 5 show that the outage probability of U_2 increases and becomes significantly very high when the mean RSI power at the relay node is increased. Increase of mean RSI degrades the SINR at R , which affects the

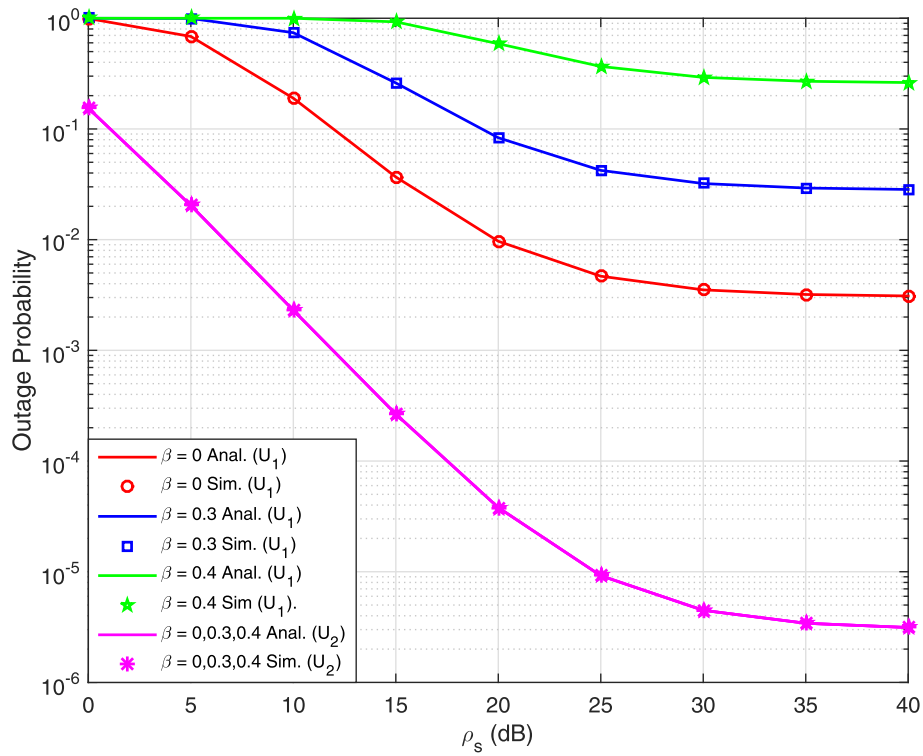


Fig. 3 Outage probability versus ρ for distinct values of β : FDR-NOMA ($\alpha_1 = 0.05$)

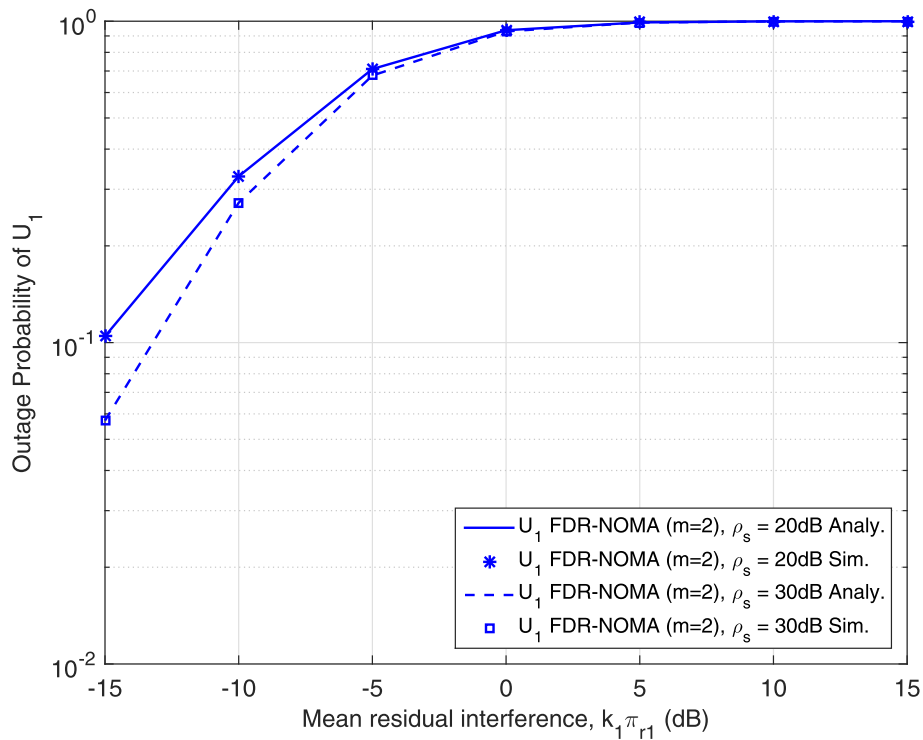
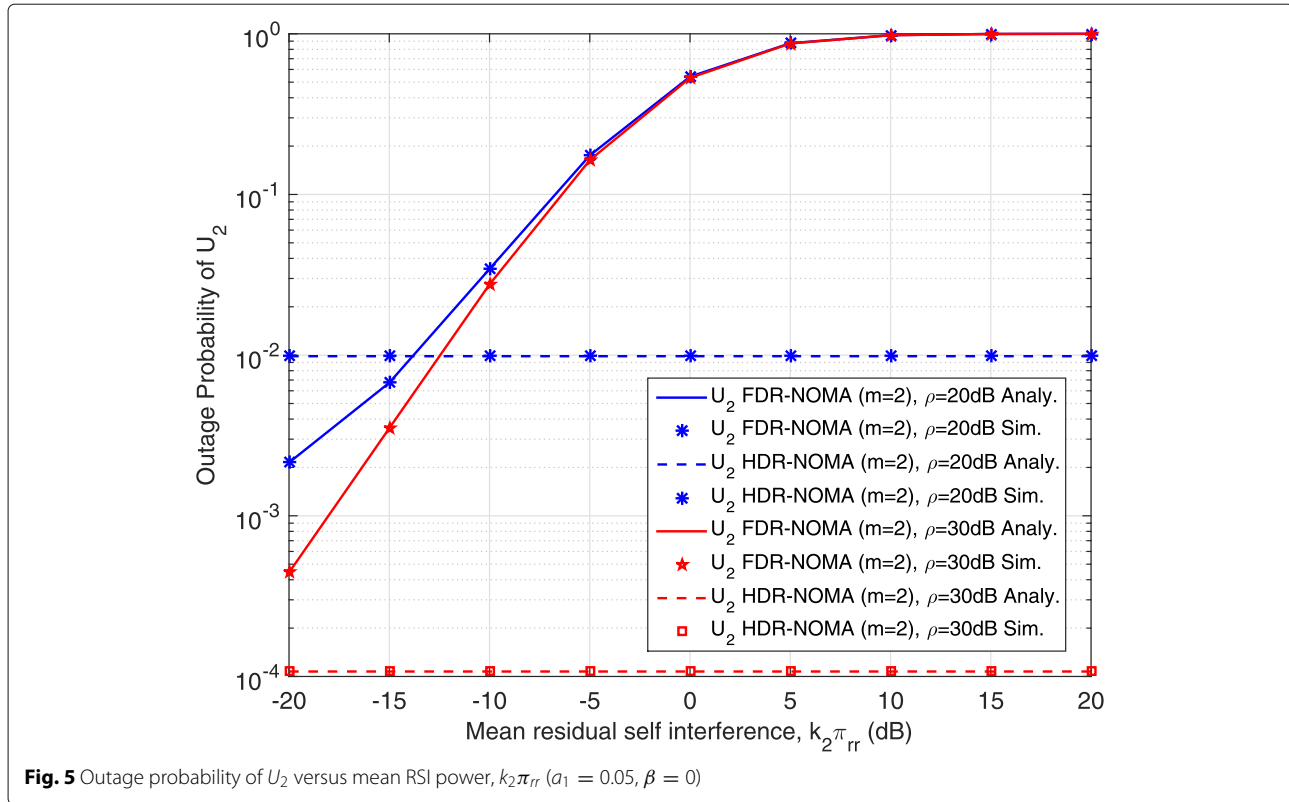


Fig. 4 Outage probability of U_1 versus mean residual interference power, $k_1\pi_{r1}$ ($\alpha_1 = 0.05$, $\beta = 0$)

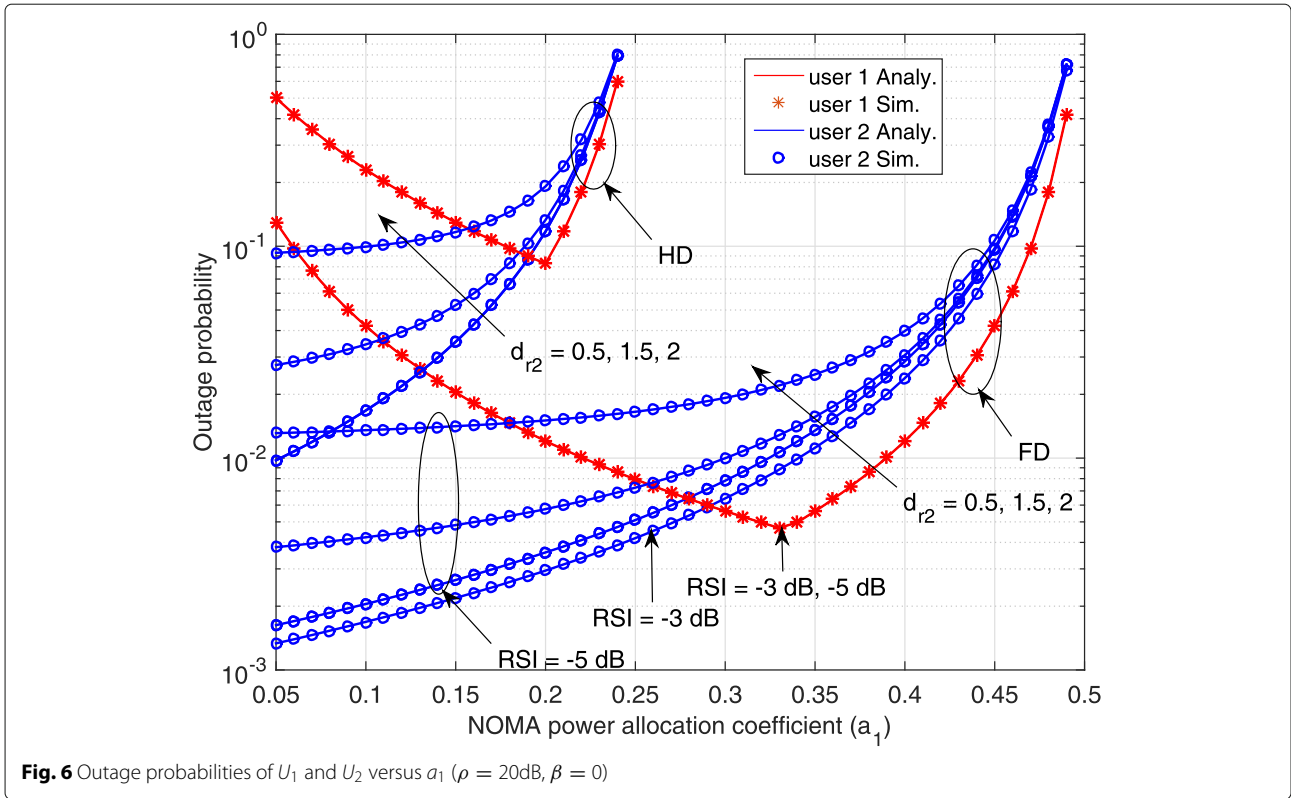


successful decoding of x_2 at R . This degrades the outage performance of U_2 , while HD relaying does not induce RSI, and thus, the outage probability of U_2 does not depend on mean RSI power in HDR-NOMA-CDRT system.

6.1 Equal outage for U_1 and U_2

Figure 6 shows the outage probability of U_1 and U_2 drawn against the NOMA power allocation coefficient a_1 . The results are shown for both HDR as well as FDR-based systems. Here, we keep $d_{s1} = 0.8$, $d_{sr} = 1.25$, $d_{r1} = 0.8$, and d_{r2} is varied along the straight line joining BS, R, and U_2 . Thus, U_2 moves away from BS while the position of U_1 is fixed. As d_{r2} increases, P_{out} of U_2 becomes higher, whereas d_{r2} does not influence P_{out} of U_1 . As a_1 increases, more power gets allocated to U_1 ; thus, P_{out} of U_1 decreases while that of U_2 increases. The outages become very high and moves towards unity when $u_2^{FD} \geq \frac{a_2}{a_1}$ for FDR-based system. Further, we can see that the outage of U_2 in FDR-based system becomes higher when RSI is increased while that of U_1 does not depend on RSI as we have seen in Fig. 2 as well. From Fig. 6, it is clear that, for certain values of a_1 (i.e., a_1^*), P_{out} of both the users can be made equal, irrespective of the location of U_2 . Table 1 depicts the details of the NOMA power allocation factor a_1^* that makes $P_{out,1} = P_{out,2}$ for FDR/HDR-NOMA-CDRT system as a function of d_{r2} . As d_{r2} is increased, a_1^*

reduces, owing to the fact that more power need to be allocated for U_2 when it moves away from BS, so as to satisfy the equal outage criterion. Furthermore, it can be seen that the a_1^* that ensures equal outage for both the users is a function of mean RSI power in FDR-based system. As the mean RSI power increases, the SINR on the BS-R link reduces which increases the outage probability of U_2 . Moreover, results given in Table 2 implies that as the I-SIC factor β is increased, a_1^* has to be increased to satisfy the equal outage criterion. This is because, an increase of β will make $P_{out,1}^{FD}$ higher; consequently, a_1^* shall be increased to meet the equal outage criterion. Thus, to ensure equal outage, a_1^* has to be reduced (i.e., a_2^* must be increased) so that more power gets allocated to U_2 's symbol at BS when the mean RSI power is increased. Since RSI is absent in HDR system, a_1^* is independent of mean RSI power. Figure 7 plots P_{out} against ρ by choosing power allocation factor a_1^* , according to the results given in Table 1 (a_1^* is calculated for each value of ρ). In this figure, results are plotted for two distinct values of d_{r2} , i.e., $d_{r2} = 0.5$, and 1.5. Further, results are shown for HDR as well as FDR systems. The results are plotted by finding a_1^* separately for each case and for each value of ρ considered. The results show that proper selection of a_1^* can make the outage probabilities of both the users equal, over the entire range of transmit power values considered.



6.2 System outage probability evaluation

Figure 8 shows the system outage probability as a function of ρ . In the low transmit power region, the system outage of FDR-NOMA-CDRT network is lower as compared to the HDR counterpart owing to the higher threshold SINR requirement for the HDR system. However, in the high transmit power region, HDR system outperforms FDR system, owing to the higher amount of mean RSI power

Table 1 NOMA coefficient a_1^* that achieves $P_{out,1} = P_{out,2}$: impact of RSI

Distance d_{r2}	RSI	a_1^* (HDR)	a_1^* (FDR)
$d_{r2} = 0.5$	-3 dB	0.19	0.28
	-5 dB	0.19	0.29
	-10 dB	0.19	0.306
	-20 dB	0.19	0.315
	-3 dB	0.185	0.256
$d_{r2} = 1.5$	-5 dB	0.185	0.27
	-10 dB	0.185	0.28
	-20 dB	0.185	0.285
	-3 dB	0.16	0.18
$d_{r2} = 2$	-5 dB	0.16	0.185
	-10 dB	0.16	0.189
	-20 dB	0.16	0.19

present in FDR system. Figure 9 shows the effect of β on system outage probability. It is evident that as the value of β increases, the system outage probability also increases. This happens owing to the fact that increases of β introduce residual interference at U_1 due to I-SIC. Thus, U_1 experience higher outage probability that increases system outage as well. Figure 10 shows the impact of RSI on the system outage of FDR-NOMA-CDRT system while Fig. 11 shows the effect of R- U_2 distance d_{r2} . The results confirm that the system outage increases with increase of RSI power owing to the fact that, as RSI power is increased, the SINR over BS-R link degrades so that the outage probability suffered by U_2 increases. Further, increase of d_{r2} increases the outage experienced by U_2 triggering the system outage to become higher. As can be seen in Figs. 10 and 11, the system outage increases either when a_1 is reduced or when a_1 is increased.

When a_1 is small, the outage probability of U_1 becomes higher, which makes the system outage also to be higher. When a_1 is increased, the outage experienced by U_2 becomes higher, which degrades the system outage. Thus,

Table 2 NOMA coefficient a_1^* that achieves $P_{out,1} = P_{out,2}$: impact of I-SIC factor β

β	0.1	0.2	0.3	0.4	0.5	0.6
a_1^* (FDR)	0.295	0.33	0.36	0.384	0.409	0.429

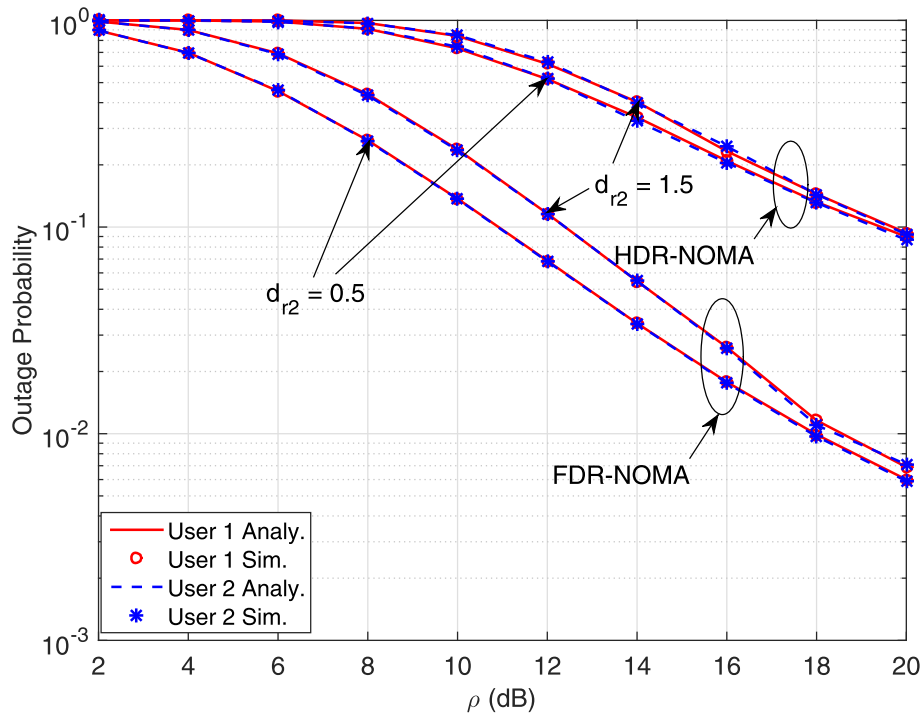


Fig. 7 Outage probabilities of U_1 and U_2 versus ρ ($a_1 = a_1^*$, $\beta = 0$)

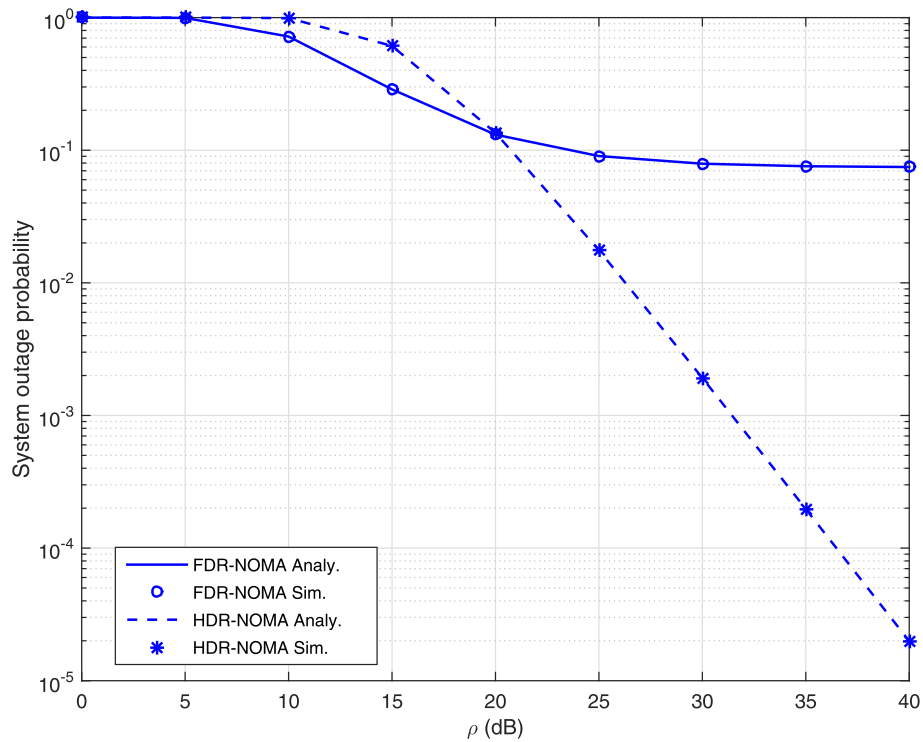


Fig. 8 System outage probability versus ρ : FDR-NOMA ($a_1 = 0.05$, $\beta = 0$)

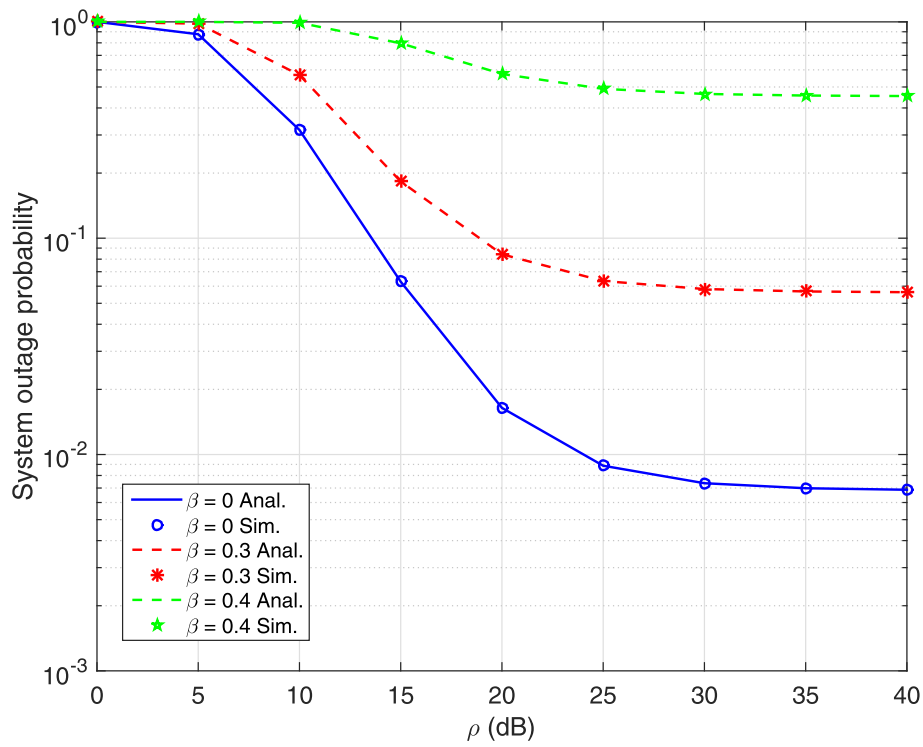


Fig. 9 System outage probability versus ρ for distinct values of β : FDR-NOMA ($a_1 = 0.05$)

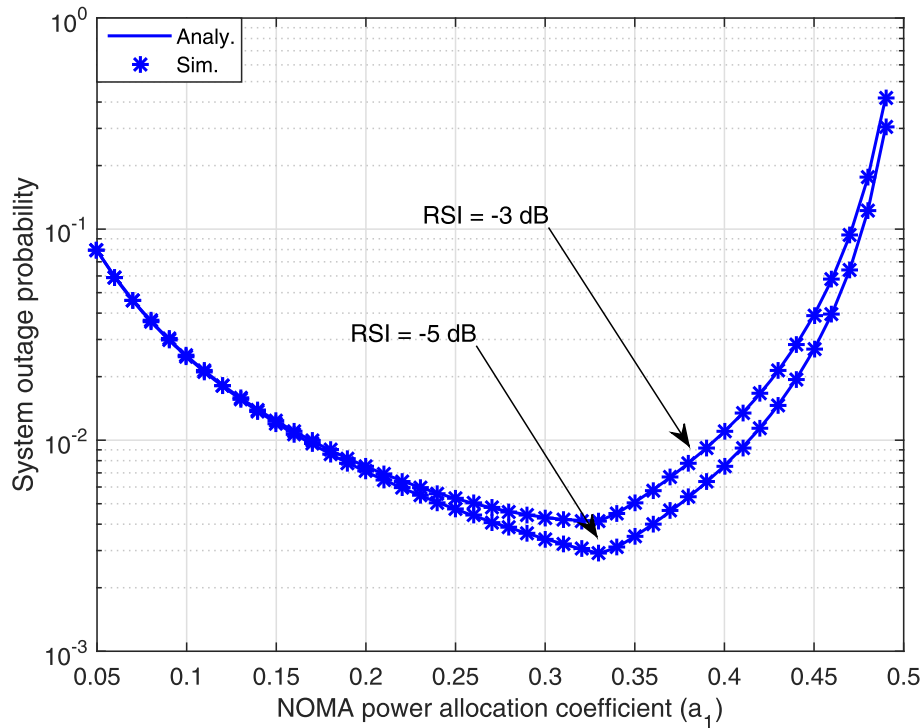
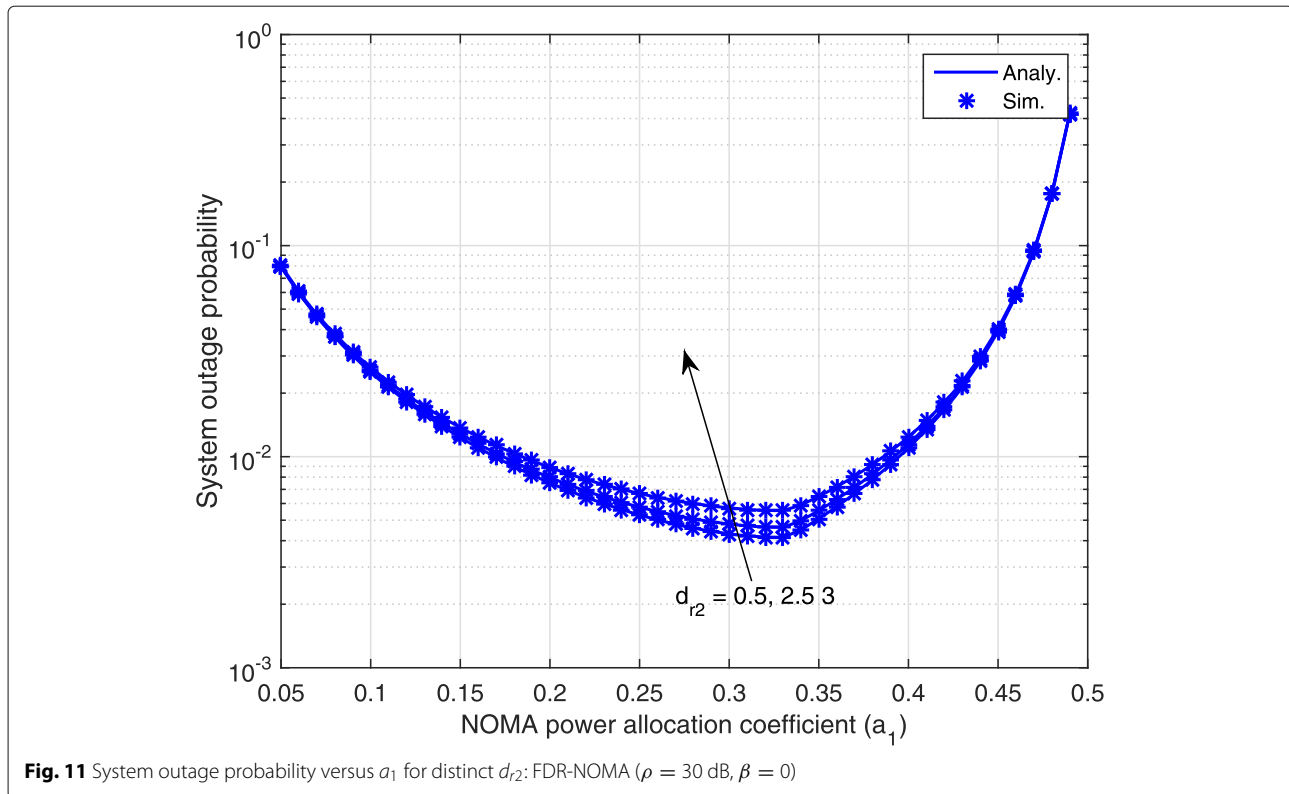


Fig. 10 System outage probability versus a_1 for distinct π_{rr} : FDR-NOMA ($\rho = 30$ dB, $\beta = 0$)



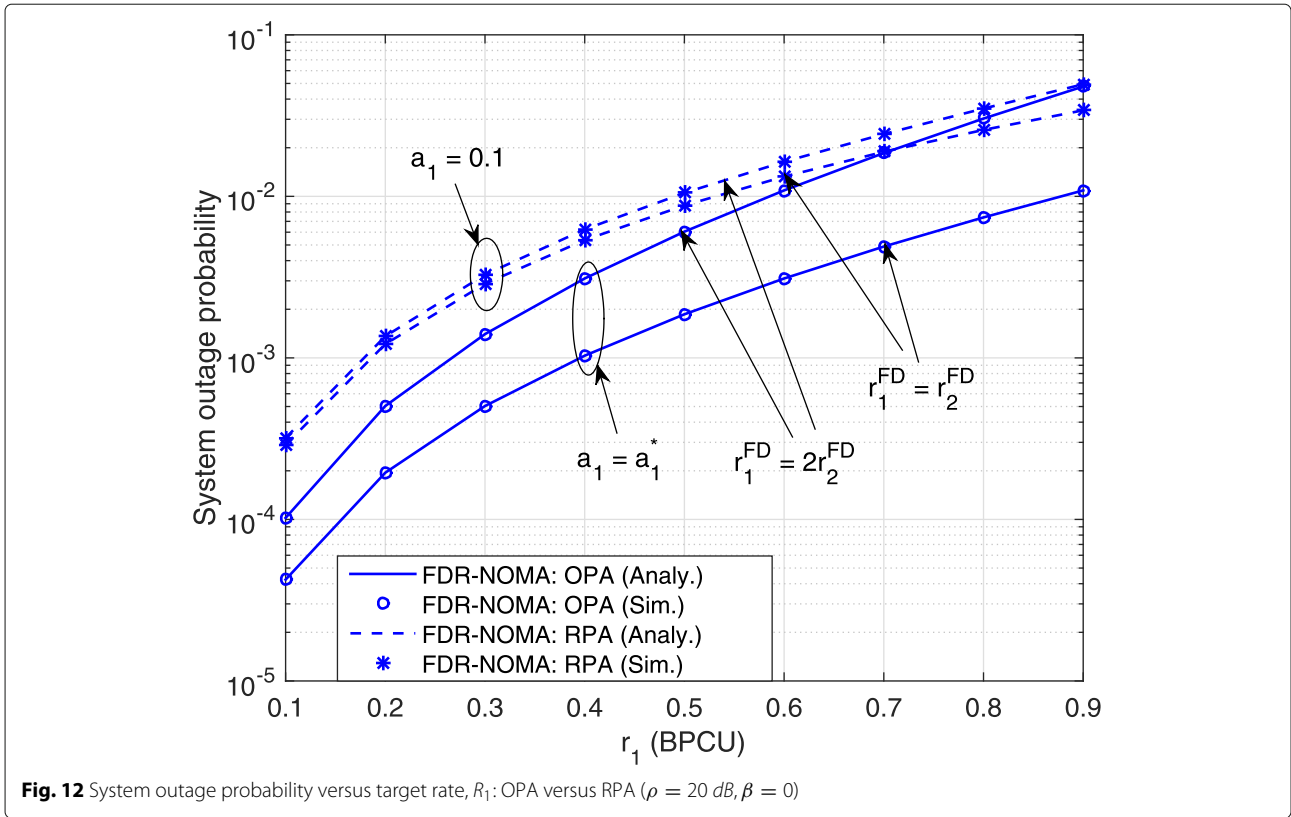
proper selection of a_1 can minimize the system outage probability.

Next, we find the optimal power allocation factor $a_{1,opt}$ and the corresponding optimal system outage probability ($P_{out,sys}^{FD,opt}$), based on the analysis described in Section 5 for FDR-NOMA-CDRT system. We also find the system outage for random power allocation (RPA) (i.e., non-optimal selection of a_1) as well. The system outage for the optimal and non-optimal schemes are shown in Fig. 12. Results show that OPA outperforms RPA significantly. With $R_1 = R_2 = 0.5$ bpcu and for the assumed set of parameters indicated in Fig. 12, OPA provides 79% improvement in system outage probability as compared to the RPA scheme. With $R_1 = 2R_2 = 0.5$ bpcu, OPA scheme leads to 42% improvement in system outage as compared to the RPA scheme. Thus, we conclude that proper selection of a_1 can improve the system outage performance of the FDR-based NOMA-CDRT network considered in this paper. Table 3 lists the numerical values of $a_{1,opt}$ that minimizes the system outage as a function of target rates R_1 and R_2 . When R_1 becomes higher, higher values for $a_{1,opt}$ has to be chosen so as to minimize $P_{out,sys}^{FD}$. A higher value for R_2 makes $a_{1,opt}$ to decrease to meet the desired objective.

6.3 Evaluation of ergodic rates of U_1 and U_2

Figures 13 and 14 respectively show the ergodic rate achieved by the users and the ergodic sum rate of the

network, for FDR-based NOMA-CDRT system. In Fig. 13, the ergodic rates corresponding to both the users are shown. The residual interference ($k_1\pi_{r1}$) and mean RSI ($k_2\pi_{rr}$) are chosen as variables. The ergodic rate of U_1 depends on $k_1\pi_{r1}$. As $k_1\pi_{r1}$ increases, ergodic rate of U_1 decreases due to higher interference at U_1 's receiver. Ergodic rate of U_1 does not depend on $k_2\pi_{rr}$, (the mean RSI power), as this quantity does not influence the SINR at U_1 . Ergodic rate of U_2 decreases as $k_2\pi_{rr}$ is increased, while $k_1\pi_{r1}$ does not have any influence on it. The impact of mean RSI ($k_2\pi_{rr}$) on the ergodic rate of U_2 becomes predominant at higher transmit power since mean RSI power is higher in the high transmit power region. Further, we can see that the ergodic rate shows a saturation behavior in the high transmit power region owing to the higher amount of interference experienced by the receivers of the users. In the high transmit power region, both the RSI ($k_2\pi_{rr}$) as well as the residual interference ($k_1\pi_{r1}$) become predominant. Accordingly, ergodic rates no longer maintains linear relation with ρ ; thus, a saturation behavior is seen. The ergodic sum rate of the system is shown in Fig. 14. Increase of residual interference at U_1 (i.e., $k_1\pi_{r1}$) and mean RSI at R (i.e., $k_2\pi_{rr}$) decreases the ergodic sum rate of the network. The degradation of ergodic sum rate is more predominant in the high transmit power region owing to the higher amount of interference in the system. Initially as the transmit power increases, the ergodic sum



rate increases; however, for larger transmit power values, it shows a saturation behavior owing to the fact that interference plays a key role in this region, and the system performance is limited by the interference. Figure 15 shows the effect of I-SIC factor β on ergodic rates of U_1 and U_2 . As described earlier, β does not influence the performance of U_2 since it does not have to implement SIC technique for decoding the message. However, increase of β increases the interference at U_1 , which degrades the achievable ergodic rate of U_1 .

Table 3 OPA factor $a_{1,opt}$ and $p_{out,sys}^{FD}$ under OPA/RPA scheme (FDR-NOMA)

(R_1, R_2)	$a_{1,opt}$	$p_{out,sys}^{FD}$ under		% improvement in system outage
		OPA	RPA ($\alpha = 0.1$)	
(0.1,0.1)	0.48	4.24×10^{-5}	2.89×10^{-4}	85.37
(0.1,0.3)	0.22	1.94×10^{-4}	3.75×10^{-4}	48.13
(0.3,0.1)	0.72	1.95×10^{-5}	0.0028	92.86
(0.3,0.3)	0.45	5.04×10^{-4}	0.0029	82.76

6.4 Comparison between NOMA and OMA

In this section, we compare the performance of FDR-NOMA-CDRT against conventional orthogonal multiple access (OMA)-based CDRT system, where communication is completed in two time slots. Here, the BS transmits the symbol x_1 to U_1 in the first time slot, which is subsequently decoded by U_1 towards the end of the first time slot. In the second time slot, the BS transmits the symbol x_2 , which is decoded and forwarded by R to U_2 . Since R operates in FD mode, simultaneous reception and transmission happens at R so that x_2 is decoded at U_2 in the same time slot with certain processing delay, i.e., time division multiple access (TDMA) is considered as the OMA scheme, with the duration of the two time slots to be equal to T sec. We consider an OMA technique where power control is considered at the BS, i.e., power allocated to x_1 is $a_1\rho_s$ and that for x_2 is $a_2\rho_s$ as in NOMA, where $a_1 + a_2 = 1$.

For a fair comparison of outage, we set the target rates for NOMA and OMA to be equal; the SINR thresholds are calculated based on this. Since OMA requires additional time slots for completing the transmission, the achievable rate under OMA gets reduced. Since the target rates for NOMA and OMA are set to be the same, the threshold SINR becomes higher for both U_1 and U_2 under OMA. Notice that when OMA is considered, the decoding of x_1 at U_1 happens in the absence of interference either due to x_2 or due to transmissions from R

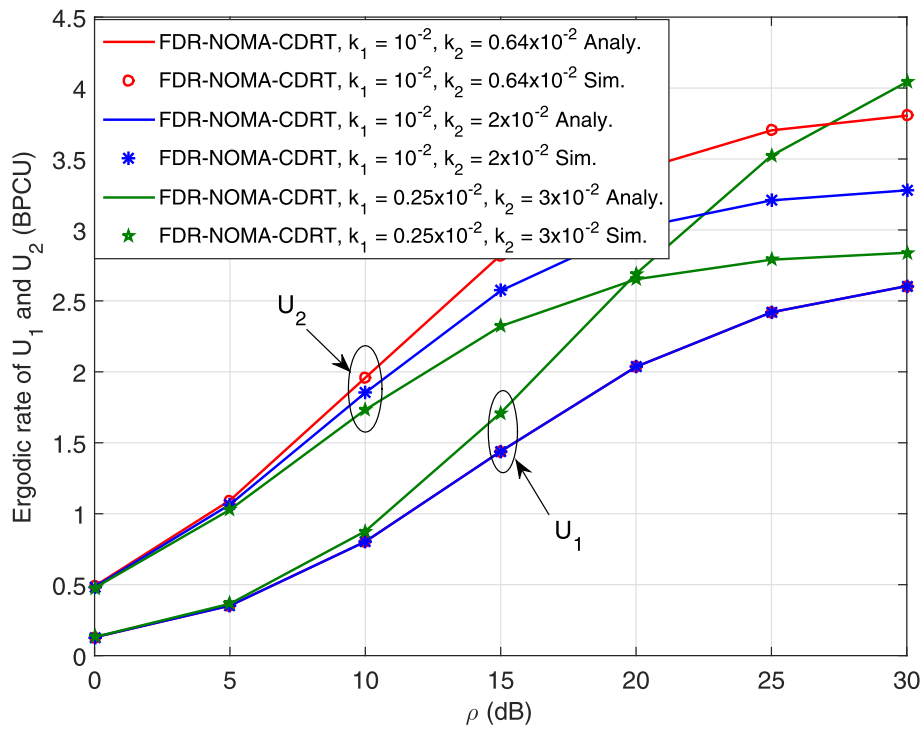


Fig. 13 Ergodic rate versus ρ ($a_1 = 0.05, \beta = 0$)

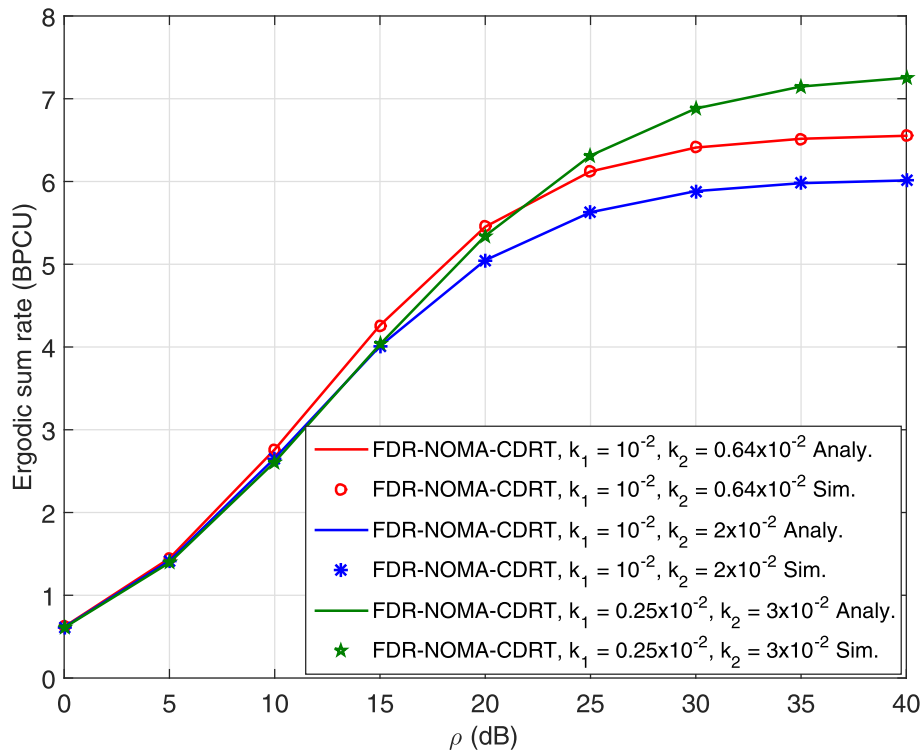
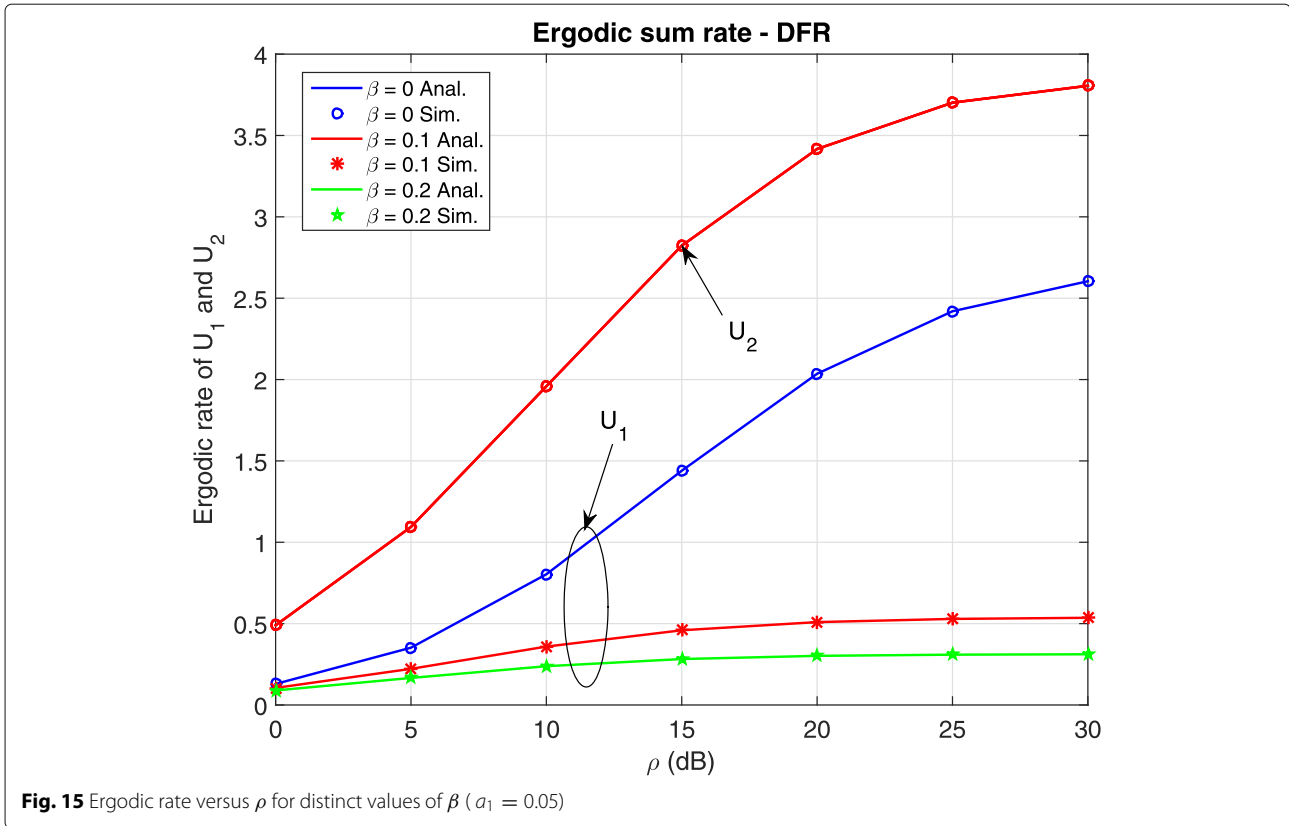


Fig. 14 Ergodic sum rate versus ρ ($a_1 = 0.05, \beta = 0$)



(since U_1 is silent during the second time slot). Figure 16 compares the outage performance of U_1 under NOMA and OMA. The results show that in the absence of any residual interference (i.e., $k_1 = 0$), the outage performance of U_1 under NOMA remains to be significantly better than that under OMA scheme considered. However, when k_1 increases, U_1 is affected by interference from R's transmission in the considered FDR-NOMA-CDRT system, which degrades the SINR at U_1 ; thus, U_1 suffers higher outage in NOMA system as compared to OMA. Figure 17 shows the corresponding results for the outage performance of U_2 . Notice that, as far as U_2 's performance is considered, NOMA outperforms OMA-based scheme for the entire range of transmit power considered. Figure 18 shows the system outage probability under NOMA and OMA. The results show that the system outage probability of FDR-NOMA-CDRT is much smaller than that of FDR-OMA-CDRT for the entire range of transmit power considered, if the residual interference is negligible at U_1 (i.e., $k_1 = 0$). However, if k_1 is non-zero, the system outage performance degrades significantly so that OMA will outperform NOMA system. As mentioned before, in the high transmit power region, HDR system performs significantly better than FDR system, owing to the enhanced RSI generated by FD operation. Further, the results shown in Fig. 19 implies that

NOMA outperforms OMA in terms of ergodic sum rate as well.

7 Conclusion

This paper considered a full-duplex-based coordinated direct and relay transmission (CDRT) system that facilitates delivery of message from a base station (BS) to two geographically separated users, i.e., a near user and a far (cell edge) user. The BS was assumed to employ power domain NOMA to transmit the messages to the users. An intermediate full-duplex relay was used to assist the message delivery to the far user. Analytical expressions for the outage probability and ergodic rates of both the users and system outage probability were derived, assuming independent non-identically distributed Nakagami fading. The impact of imperfect SIC was considered for the analysis. The outage probability experienced by the near user was observed to be higher than that experienced by far user. Further, it was established that proper selection of NOMA power allocation coefficient at the BS can lead to equal outage probabilities for both the users. Finally, analytical expression for the optimal power allocation (OPA) coefficient at the BS that minimizes the system outage probability was also derived. Through extensive numerical and simulation investigations, it was established that selection of OPA coefficient according to the criterion

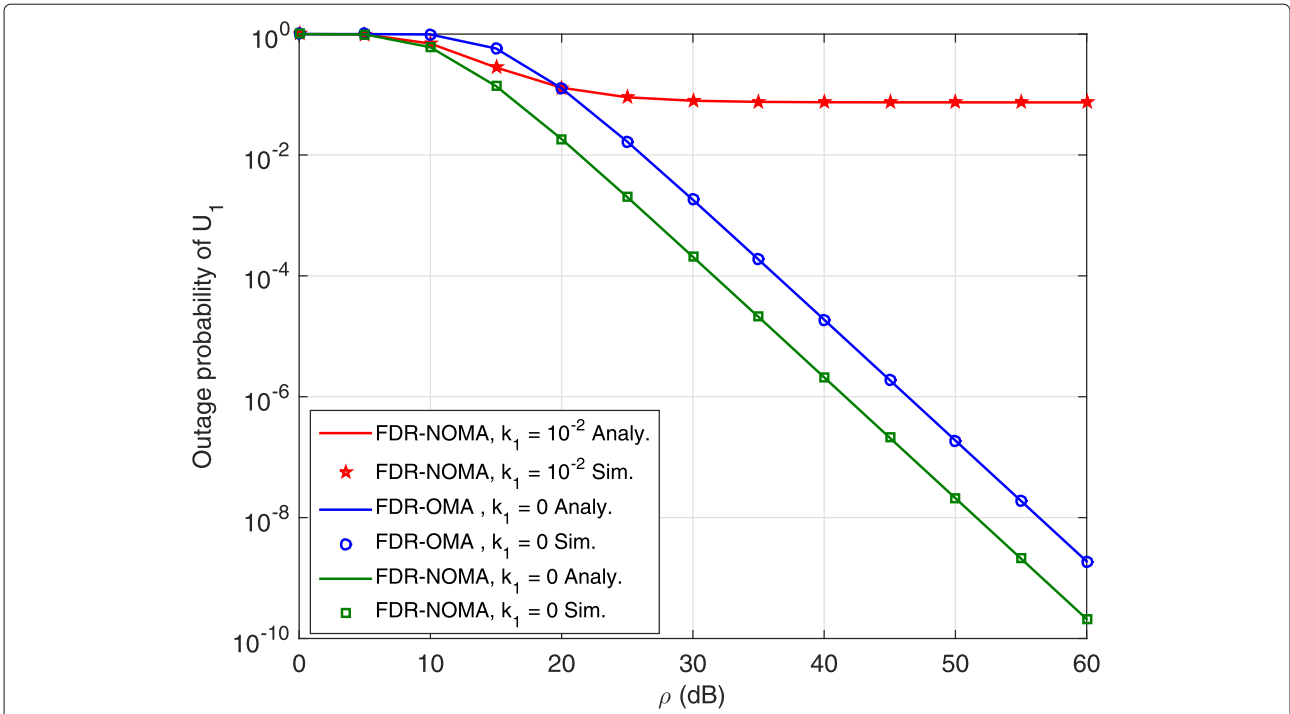


Fig. 16 Outage probability of U_1 versus ρ : NOMA and OMA schemes ($a_1 = 0.05, \beta = 0$)

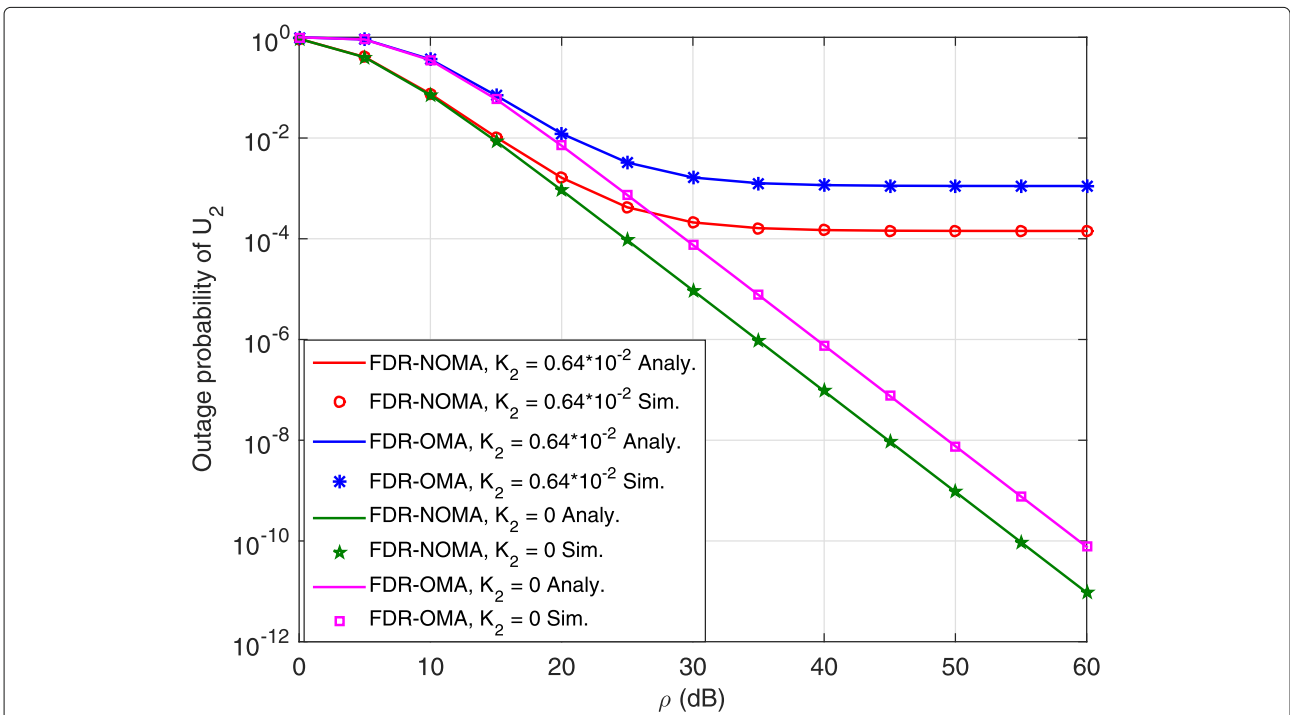


Fig. 17 Outage probability of U_2 versus ρ : NOMA and OMA schemes ($a_1 = 0.05, \beta = 0$)

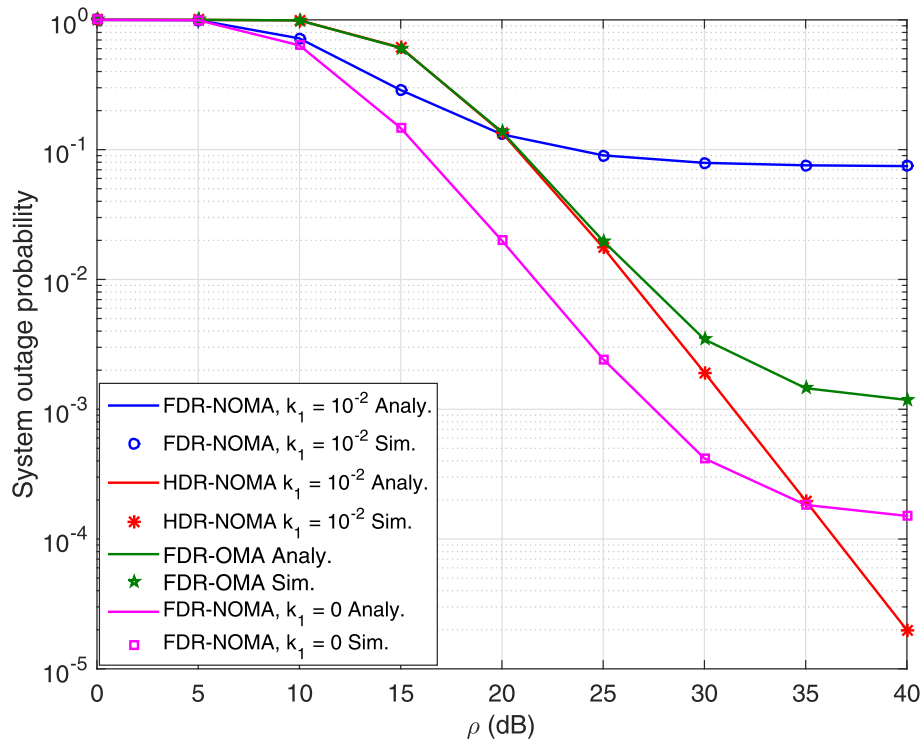


Fig. 18 System outage probability versus ρ : NOMA and OMA schemes ($a_1 = 0.05, \beta = 0$)

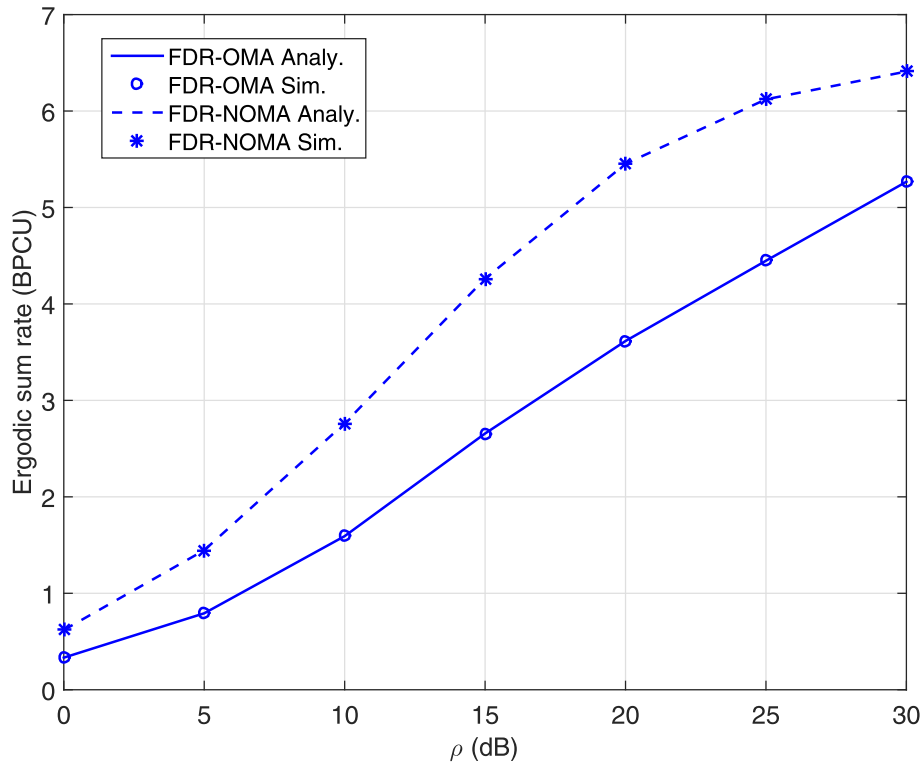


Fig. 19 Ergodic sum rate versus ρ : NOMA and OMA schemes ($a_1 = 0.05, \beta = 0$)

given in the paper can significantly improve the system outage performance of the considered FDR-NOMA CDRT network, as compared to random power allocation at the BS.

Appendix A

Derivation of (18):

Consider the definition of $P_{out,1}^{FD}$ given in (17). Substituting the expressions for Γ_{12} and Γ_{11} in (17), we get

$$P_{out,1}^{FD} = 1 - Pr \left\{ \frac{|h_{s1}|^2 \rho_s a_2}{|h_{s1}|^2 \rho_s a_1 + |\hat{h}_{r1}|^2 \rho_r + 1} \geq u_2^{FD}, \frac{|h_{s1}|^2 \rho_s a_1}{|h_{s1}|^2 \rho_s \beta a_2 + |\hat{h}_{r1}|^2 \rho_r + 1} \geq u_1^{FD} \right\} \quad (37a)$$

$$= 1 - Pr \left\{ |h_{s1}|^2 \geq \frac{u_2^{FD} (|\hat{h}_{r1}|^2 \rho_r + 1)}{(a_2 - a_1 u_2^{FD}) \rho_s}, |h_{s1}|^2 \geq \frac{u_1^{FD} (|\hat{h}_{r1}|^2 \rho_r + 1)}{(a_1 - a_2 u_1^{FD}) \rho_s} \right\} \quad (37b)$$

$$= 1 - Pr \left\{ |h_{s1}|^2 \rho_s \geq \frac{1}{\phi} (|\hat{h}_{r1}|^2 \rho_r + 1) \right\} \quad (37b)$$

where $\phi = \min \left(\frac{a_2 - u_2^{FD} a_1}{u_2^{FD}}, \frac{a_1 - \beta a_2 u_1^{FD}}{u_1^{FD}} \right)$. The CDF and PDF of $|h_{ij}|^2$ are given in (2a) and (2b), respectively. Utilizing these expressions, (37b) can be simplified as follows:

$$P_{out,1}^{FD} = 1 - \int_0^\infty e^{-\left(\frac{y\rho_r+1}{\phi\rho_s\beta s_1}\right)} \sum_{j=0}^{m_{s1}-1} \frac{1}{j!} \left(\frac{y\rho_r+1}{\phi\rho_s\beta s_1}\right)^j (k_1\beta_{r1})^{-m_{r1}} \frac{y^{m_{r1}-1}}{\Gamma(m_{r1})} e^{-\frac{y}{\beta_{r1}k_1}} dy \quad (38a)$$

$$= 1 - e^{-\frac{1}{\phi\rho_s\beta s_1}} \frac{(k_1\beta_{r1})^{-m_{r1}}}{\Gamma(m_{r1})} \sum_{j=0}^{m_{s1}-1} \frac{1}{j!} \left(\frac{\rho_r}{\phi\rho_s\beta s_1}\right)^j \int_0^\infty e^{-\frac{y\rho_r}{\phi\rho_s\beta s_1}} e^{-\frac{y}{\beta_{r1}k_1}} y^{m_{r1}-1} \left(\frac{\rho_r y + 1}{\phi\rho_s\beta s_1}\right)^j dy \quad (38a)$$

$$= 1 - e^{-\frac{1}{\phi\rho_s\beta s_1}} \frac{(k_1\beta_{r1})^{-m_{r1}}}{\Gamma(m_{r1})} \sum_{j=0}^{m_{s1}-1} \frac{1}{j!} \left(\frac{\rho_r}{\phi\rho_s\beta s_1}\right)^j \sum_{k=0}^j {}^j C_k \left(\frac{1}{\rho_r}\right)^{j-k} \times \int_0^\infty e^{-\left(\frac{\rho_r}{\phi\rho_s\beta s_1} + \frac{1}{\beta_{r1}k_1}\right)y} y^{m_{r1}+k-1} dy \quad (38b)$$

where $u_2^{FD} < \frac{a_2}{a_1}$ or $u_1^{FD} < \frac{a_1}{\beta a_2}$. Notice that (38b) is obtained from (38a) after using binomial expansion for term $(y+1/\rho_r)^j$, i.e., $(y+1/\rho_r)^j = \sum_{k=0}^j {}^j C_k y^k (1/\rho_r)^{j-k}$. Now, the integral in (38b) can be simplified by using [40] (3.351.3).

Upon simplification, the final expression for $P_{out,1}^{FD}$ can be obtained as in (18). Further, we can see that when $u_2^{FD} \geq \frac{a_2}{a_1}$ or when $u_1^{FD} \geq \frac{a_1}{\beta a_2}$, the probability term on the RHS of (37a) will become zero so that $P_{out,1}$ tends to unity.

Appendix B

Derivation of (20):

Consider the definition of $P_{out,2}^{FD}$ given in (19). Substituting the expressions for Γ_{r2} and Γ_{22} as given in (5) and (8) in (19), we get the following:

$$P_{out,2}^{FD} = 1 - Pr \left\{ \frac{|h_{sr}|^2 \rho_s a_2}{|h_{sr}|^2 \rho_s a_1 + |h_{rr}|^2 \rho_r + 1} \geq u_2^{FD}, |h_{r2}|^2 \rho_r \geq u_2^{FD} \right\} \quad (39a)$$

$$= 1 - Pr \left\{ |h_{sr}|^2 \rho_s \geq \frac{u_2^{FD}}{a_2 - u_2^{FD} a_1} (|h_{rr}|^2 \rho_r + 1), |h_{r2}|^2 \rho_r \geq u_2^{FD} \right\} \quad (39a)$$

$$= 1 - Pr \left\{ |h_{sr}|^2 \rho_s \geq \frac{(|h_{rr}|^2 \rho_r + 1)}{\psi} \right\} \quad (39b)$$

$$\times Pr \left\{ |h_{r2}|^2 \rho_r \geq u_2^{FD} \right\} \triangleq 1 - (A_0 \times B_0) \quad (39c)$$

where $\psi = \frac{a_2 - u_2^{FD} a_1}{u_2^{FD}}$. Notice that (39b) is written under the assumption that the channel power gains $|h_{sr}|^2$ and $|h_{r2}|^2$ are independent. Now, A_0 and B_0 can be evaluated by utilizing the expressions for the CDF and PDF of $|h_{ij}|^2$ given in (2). Accordingly, we proceed as follows:

$$A_0 = Pr \left\{ |h_{sr}|^2 \geq \frac{|h_{rr}|^2 \rho_r + 1}{\psi \rho_s} \right\} = \int_0^\infty e^{-\left(\frac{y\rho_r+1}{\psi\rho_s\beta_{sr}}\right)} \sum_{j=0}^{m_{sr}-1} \frac{1}{j!} \left(\frac{y\rho_r+1}{\psi\rho_s\beta_{sr}}\right)^j (k_2\beta_{rr})^{-m_{rr}} \frac{y^{m_{rr}-1}}{\Gamma(m_{rr})} e^{-\frac{y}{\beta_{rr}k_2}} dy \quad (40)$$

$$= e^{-\frac{1}{\psi\rho_s\beta_{sr}}} \frac{(k_2\beta_{rr})^{-m_{rr}}}{\Gamma(m_{rr})} \sum_{j=0}^{m_{sr}-1} \frac{1}{j!} \int_0^\infty e^{-\left(\frac{\rho_r}{\psi\rho_s\beta_{sr}} + \frac{1}{\beta_{rr}k_2}\right)y} y^{m_{rr}-1} \left(\frac{y\rho_r+1}{\psi\rho_s\beta_{sr}}\right)^j dy \quad (40)$$

Applying binomial expansion for the term $(y + (1/\rho_r))^j$; we get the following equation:

$$A_0 = e^{-\frac{1}{\psi\rho_s\beta_{sr}}} \frac{(k_2\beta_{rr})^{-m_{rr}}}{\Gamma(m_{rr})} \sum_{j=0}^{m_{sr}-1} \frac{1}{j!} \left(\frac{\rho_r}{\psi\rho_s\beta_{sr}} \right)^j \times \sum_{k=0}^j {}^j C_k \left(\frac{1}{\rho_r} \right)^{j-k} \times \int_0^\infty e^{-\left(\frac{\rho_r}{\psi\rho_s\beta_{sr}} + \frac{1}{\beta_{rr}k_2}\right)y} y^{k+m_{rr}-1} dy \quad (41)$$

Now, the integral in (41) can be simplified by using [40] (3.351.3). Accordingly, the final expression for A_0 can be obtained as follows:

$$A_0 = e^{-\frac{1}{\psi\rho_s\beta_{sr}}} \frac{(k_2\beta_{rr})^{-m_{rr}}}{\Gamma(m_{rr})} \sum_{j=0}^{m_{sr}-1} \frac{1}{j!} \left(\frac{\rho_r}{\psi\rho_s\beta_{sr}} \right)^j \times \sum_{k=0}^j {}^j C_k \left(\frac{1}{\rho_r} \right)^{j-k} (m_{rr} + k - 1)! \times \left(\frac{\rho_r}{\psi\rho_s\beta_{sr}} + \frac{1}{\beta_{rr}k_2} \right)^{-m_{rr}-k} \quad (42)$$

Further, B_0 is determined as follows:

$$B_0 = Pr\{|h_{r2}|^2 \rho_r \geq u_2^{FD}\} = Pr\left\{|h_{r2}|^2 \geq \frac{u_2^{FD}}{\rho_r}\right\} = e^{-\left(\frac{u_2^{FD}}{\rho_r\beta_{r2}}\right)} \sum_{i=0}^{m_{r2}-1} \frac{1}{i!} \left(\frac{u_2^{FD}}{\rho_r\beta_{r2}} \right)^i \quad (43)$$

The final expression in (20) can be obtained by substituting (42) and (43) in (39c). Further, when $u_2^{FD} \geq \frac{a_2}{a_1}$, A_0 will become zero so that $P_{out,2}^{FD}$ tends to be unity. Proposition 2 is thus proved.

Appendix C

Derivation of (21f):

Consider the expression for $P_{out,sys}^{FD}$ given in (21e).

$$\text{Let } C_0 = 1 - Pr\left\{|h_{s1}|^2 \geq \frac{1}{\phi\rho_s} (|\hat{h}_{r1}|^2 \rho_r + 1)\right\}; A_0 = Pr\left\{|h_{sr}|^2 \geq \frac{|\hat{h}_{rr}|^2 \rho_r + 1}{\psi\rho_s}\right\}; \text{ and } B_0 = Pr\left\{|h_{r2}|^2 \geq \frac{u_2^{FD}}{\rho_r}\right\}.$$

Accordingly, referring to (21e), we write $P_{out,sys}^{FD} \triangleq (1 - [C_0 \times A_0 \times B_0])$. From A, $C_0 = 1 - P_{out,1}^{FD}$. Further, A_0 and B_0 are given by (42) and (43) of B. Combining these equations, $P_{out,sys}^{FD}$ can be obtained as given in (21f). However, notice that if either $u_2^{FD} \geq a_2/a_1$ or $u_1^{FD} \geq a_1/\beta a_2$, C_0 will becomes zero so that $P_{out,sys}^{FD}$ tends to unity. Proposition 3 is thus proved.

Appendix D

Derivation of (22b):

The CDF of Γ_{11} , i.e., $F_{\Gamma_{11}}(x)$ is determined as follows:

$$F_{\Gamma_{11}}(x) = 1 - Pr\left(\frac{|h_{s1}|^2 \rho_s a_1}{|h_{s1}|^2 \rho_s \beta a_2 + |\hat{h}_{r1}|^2 \rho_r + 1} > x\right) = 1 - Pr\left(|h_{s1}|^2 > \frac{x}{\rho_s(a_1 - \beta a_2 x)} (|\hat{h}_{r1}|^2 \rho_r + 1)\right) = 1 - \int_{y=0}^\infty e^{-\frac{(\rho_r y + 1)x}{\rho_s(a_1 - \beta a_2 x)\beta_{s1}}} \sum_{j=0}^{m_{s1}-1} \frac{1}{j!} \left(\frac{(\rho_r y + 1)x}{\rho_s(a_1 - \beta a_2 x)\beta_{s1}} \right)^j \frac{(k_1\beta_{r1})^{-m_{r1}}}{\Gamma(m_{r1})} e^{-\frac{y}{\beta_{r1}k_1}} y^{m_{r1}-1} dy = 1 - \frac{(k_1\beta_{r1})^{-m_{r1}}}{\Gamma(m_{r1})} \sum_{j=0}^{m_{s1}-1} \frac{1}{j!} \left(\frac{x}{\rho_s(a_1 - \beta a_2 x)\beta_{s1}} \right)^j e^{-\frac{x}{\rho_s(a_1 - \beta a_2 x)}} \int_{y=0}^\infty e^{-\left(\frac{x\rho_r}{\rho_s(a_1 - \beta a_2 x)\beta_{s1}} + \frac{1}{\beta_{r1}k_1}\right)y} y^{m_{r1}-1} \times (y\rho_r + 1)^j dy \quad (44)$$

Notice that (44) is obtained by utilizing the CDF and PDF expression for $|h_{ij}|^2$ given in (2). By using binomial expansion for $(y + (1/\rho_r))^j$ and utilizing [40] (3.351.3), (44) can be evaluated as,

$$F_{\Gamma_{11}}(x) = 1 - \frac{(k_1\beta_{r1})^{-m_{r1}}}{\Gamma(m_{r1})} \sum_{j=0}^{m_{s1}-1} \frac{1}{j!} \left(\frac{x}{\rho_s(a_1 - \beta a_2 x)\beta_{s1}} \right)^j \times e^{-\frac{x}{\rho_s(a_1 - \beta a_2 x)}} \sum_{k=0}^j {}^j C_k \left(\frac{1}{\rho_r} \right)^{j-k} (m_{r1} + k - 1)! \times \left(\frac{x\rho_r}{\rho_s(a_1 - \beta a_2 x)\beta_{s1}} + \frac{1}{\beta_{r1}k_1} \right)^{-m_{r1}-k} \quad (45)$$

Substituting (45) in (22a), $E_{[R_1]}^{[FD]}$ can be computed using the following expression:

$$E_{[R_1]}^{[FD]} = \frac{1}{\ln 2} \frac{(k_1\beta_{r1})^{-m_{r1}}}{\Gamma(m_{r1})} \sum_{j=0}^{m_{s1}-1} \frac{1}{j!} \sum_{k=0}^j {}^j C_k \left(\frac{1}{\rho_r} \right)^{j-k} (m_{r1} + k - 1)! \times \int_{x=0}^{\frac{a_1}{\beta a_2}} e^{-\frac{x}{\rho_s(a_1 - \beta a_2 x)\beta_{s1}}} \left(\frac{x\rho_r}{\rho_s(a_1 - \beta a_2 x)\beta_{s1}} \right)^j \left(\frac{x\rho_r}{\rho_s(a_1 - \beta a_2 x)\beta_{s1}} + \frac{1}{\beta_{r1}k_1} \right)^{-m_{r1}-k} \frac{dx}{1+x} \quad (46)$$

It is difficult to find a closed form expression for the integral term in (46), and hence, we can apply the Gaussian-Chebyshev quadrature method [41]. The basic formula used in Gaussian-Chebyshev quadrature method is given as

$$\int_{-1}^1 \frac{f(x)}{\sqrt{1-x^2}} dx \approx \frac{\pi}{N} \sum_{n=1}^N f \left[\cos \left(\frac{2n-1}{2N} \pi \right) \right] \quad (47)$$

where N is an accuracy-complexity trade-off parameter. To use (47), we substitute $x = \frac{1}{2} \frac{a_1}{\beta a_2} (1 + \phi_n)$ (where $\phi_n = \cos(\frac{(2n-1)\pi}{2N})$) in (46). Larger N leads to a more accurate approximation at the cost of higher computational complexity. The integral expression in (46) can be simplified to a form similar to (47). Thereafter, $E_{R_1}^{FD}$ can be obtained as given in (22b) by utilizing (47).

Appendix E

Derivation of (23b):

To derive the expression for $E_{R_2}^{FD}$ using (23a), we find the CDF of Y as follows:

$$\begin{aligned} F_Y(y) &= P_r(\min\{\Gamma_{12}, \Gamma_{r2}, \Gamma_{22}\} \leq y) \\ &= 1 - P_r(\Gamma_{12} > y)P_r(\Gamma_{r2} > y)P_r(\Gamma_{22} > y) \\ &= 1 - [A_1 \times A_2 \times A_3] \end{aligned} \tag{48}$$

Notice that (48) is obtained under the assumption that the links in the network experience i.n.i.d. fading. Now, A_1, A_2 and A_3 are determined as follows by utilizing the CDF/PDF expressions for $|h_{ij}|^2$ given in (2).

$$\begin{aligned} A_1 &= P_r(\Gamma_{12} > y) \\ &= P_r\left(\frac{|h_{s1}|^2 \rho_s a_2}{|h_{s1}|^2 \rho_s a_1 + |\hat{h}_{r1}|^2 \rho_r + 1} > y\right) \\ &= \int_{z=0}^{\infty} P_r\left(|h_{s1}|^2 > \frac{y(z\rho_r + 1)}{\rho_s(a_2 - a_1 y)}\right) f_{|\hat{h}_{r1}|^2}(z) dz \end{aligned} \tag{49}$$

Recall that the power gain $|h_{ij}|^2$ have Gamma PDF. Accordingly, we use the CDF/PDF expression given in (2) for evaluating (49). Thus, we get

$$\begin{aligned} A_1 &= \int_{z=0}^{\infty} e^{-\frac{y(z\rho_r + 1)}{\rho_s(a_2 - a_1 y)\beta_{s1}}} \sum_{j=0}^{m_{s1}-1} \frac{1}{j!} \left(\frac{y(z\rho_r + 1)}{\rho_s(a_2 - a_1 y)\beta_{s1}}\right)^j \\ &\quad \frac{(k_1 \beta_{r1})^{-m_{r1}}}{\Gamma(m_{r1})} z^{m_{r1}-1} e^{-\frac{z}{\beta_{r1} k_1}} dz \\ &= e^{-\frac{y}{\rho_s(a_2 - a_1 y)\beta_{s1}}} \sum_{j=0}^{m_{s1}-1} \frac{1}{j!} \left(\frac{y}{\rho_s(a_2 - a_1 y)\beta_{s1}}\right)^j \frac{(k_1 \beta_{r1})^{-m_{r1}}}{\Gamma(m_{r1})} \\ &\quad \times \int_{z=0}^{\infty} e^{-\frac{yz\rho_r}{\rho_s(a_2 - a_1 y)\beta_{s1}}} (z\rho_r + 1)^j z^{m_{r1}-1} e^{-\frac{z}{\beta_{r1} k_1}} dz \end{aligned} \tag{50}$$

To simplify (50), we invoke binomial theorem and further use the result reported in [40] (3.351.3). Thus, we get

$$\begin{aligned} A_1 &= e^{-\frac{y}{\rho_s(a_2 - a_1 y)\beta_{s1}}} \frac{(k_1 \beta_{r1})^{-m_{r1}}}{\Gamma(m_{r1})} \sum_{j=0}^{m_{s1}-1} \\ &\quad \frac{1}{j!} \left(\frac{y\rho_r}{\rho_s(a_2 - a_1 y)\beta_{s1}}\right)^j \sum_{k=0}^j {}^j C_k \left(\frac{1}{\rho_r}\right)^{j-k} \\ &\quad \times (m_{r1} + k - 1)! \left(\frac{y\rho_r}{\rho_s(a_2 - a_1 y)\beta_{s1}} + \frac{1}{\beta_{r1} k_1}\right)^{-m_{r1}-k} \end{aligned} \tag{51}$$

By following similar procedure, A_2 and A_3 can be determined as follows:

$$\begin{aligned} A_2 &= P_r(\Gamma_{r2} > y) \\ &= P_r\left(\frac{|h_{sr}|^2 \rho_s a_2}{|h_{sr}|^2 \rho_s a_1 + |h_{rr}|^2 \rho_r + 1} > y\right) \\ &= e^{-\frac{y}{\rho_s(a_2 - a_1 y)\beta_{sr}}} \frac{(k_2 \beta_{rr})^{-m_{rr}}}{\Gamma(m_{rr})} \sum_{l=0}^{m_{sr}-1} \frac{1}{l!} \left(\frac{y\rho_r}{\rho_s(a_2 - a_1 y)\beta_{sr}}\right)^l \\ &\quad \sum_{p=0}^l {}^l C_p \left(\frac{1}{\rho_r}\right)^{l-p} \\ &\quad \times (m_{sr} + p - 1)! \left(\frac{y\rho_r}{\rho_s(a_2 - a_1 y)\beta_{sr}} + \frac{1}{\beta_{rr} k_2}\right)^{-m_{sr}-p} \end{aligned} \tag{52}$$

$$\begin{aligned} A_3 &= P_r(|h_{r2}|^2 \rho_r > y) \\ &= P_r\left(|h_{r2}|^2 > \frac{y}{\rho_r}\right) \\ &= e^{-\frac{y}{\rho_r \beta_{r2}}} \sum_{q=0}^{m_{r2}-1} \frac{1}{q!} \left(\frac{y}{\rho_r \beta_{r2}}\right)^q \end{aligned} \tag{53}$$

Substituting (51) - (53) in (48), we get $F_Y(y)$. Substituting the expression for $F_Y(y)$ in (23a) and rearranging, $E_{R_2}^{FD}$ can be obtained as:

$$\begin{aligned} E_{R_2}^{FD} &= \frac{(k_1 \beta_{r1})^{-m_{r1}}}{\Gamma(m_{r1})} \sum_{j=0}^{m_{s1}-1} \frac{1}{j!} \sum_{k=0}^j {}^j C_k \left(\frac{1}{\rho_r}\right)^{j-k} \\ &\quad (m_{r1} + k - 1)! \frac{(k_2 \beta_{rr})^{-m_{rr}}}{\Gamma(m_{rr})} \end{aligned}$$

$$\begin{aligned}
& \times \sum_{l=0}^{m_{sr}-1} \frac{1}{l!} \sum_{p=0}^l C_p \left(\frac{1}{\rho_r} \right)^{l-p} (m_{rr} + p - 1)! \\
& \sum_{q=0}^{m_{r2}-1} \frac{1}{q!} \times \frac{1}{\ln 2} \\
& \times \int_{y=0}^{a_2/a_1} e^{-\frac{y}{\rho_s(a_2-a_1y)\beta_{s1}}} \left(\frac{y\rho_r}{\rho_s(a_2-a_1y)\beta_{s1}} + \frac{1}{\beta_{r1}k_1} \right)^{-m_{r1}-k} \\
& \times \left(\frac{y\rho_r}{\rho_s(a_2-a_1y)\beta_{s1}} \right)^j e^{-\frac{y}{\rho_s(a_2-a_1y)\beta_{sr}}} \left(\frac{y\rho_r}{\rho_s(a_2-a_1y)\beta_{sr}} \right)^l \\
& \times \left(\frac{y\rho_r}{\rho_s(a_2-a_1y)\beta_{sr}} + \frac{1}{\beta_{rr}k_2} \right)^{-m_{rr}-p} \\
& e^{-\frac{y}{\rho_r\beta_{r2}}} \left(\frac{y}{\rho_r\beta_{r2}} \right)^q \frac{1}{1+y} dy \quad (54)
\end{aligned}$$

To evaluate integral term in (54), we make use of the Gaussian-Chebyshev quadrature method [41]. First of all, we convert the integral in (54) into a form similar to (47) by substituting $y = \frac{1}{2} \frac{a_2}{a_1} (1 + \phi_n)$. Thereafter, $E_{R_2}^{FD}$ can be obtained as in (23b) by utilizing (47).

Abbreviations

AWGN: Additive white Gaussian noise; BS: Base station; CDF: Cumulative distribution function; CDRT: Coordinated direct and relay transmission; DF: Decode and Forward; FD: Full duplex; FDR: Full-duplex relay; HD: Half duplex; HDR: Half-duplex relay; NOMA: Non-orthogonal multiple access; OMA: Orthogonal multiple access; OPA: Optimal power allocation; PDF: Probability density function; RSI: Residual self interference; SI: Self interference; SIC: Self interference cancelation; SINR: Signal to interference plus noise ratio; SNR: Signal to interference ratio; TDMA: Time division multiple access

Acknowledgements

Not applicable.

Authors' contributions

All authors have contributed to this research work. Both authors have read and approved the final manuscript.

Authors' information

Not applicable.

Funding

Not applicable.

Availability of data and materials

Not applicable.

Competing interests

The authors declare that they have no competing interests.

Received: 29 August 2019 Accepted: 18 December 2019

Published online: 23 January 2020

References

1. S. R. Islam, N. Avazov, O. A. Dobre, K.-S. Kwak, Power-domain non-orthogonal multiple access (noma) in 5G systems: potentials and challenges. *IEEE Commun. Surv. Tutor.* **19**(2), 721–742 (2017)
2. Z. Ding, X. Lei, G. K. Karagiannidis, R. Schober, J. Yuan, V. Bhargava, A survey on non-orthogonal multiple access for 5G networks: research challenges and future trends. *IEEE J. Sel. Areas Commun.* **35**, 10 (2017)
3. Z. Ding, M. Peng, H. V. Poor, Cooperative non-orthogonal multiple access in 5G systems. *IEEE Commun. Lett.* **19**(8), 1462–1465 (2015)
4. J.-B. Kim, I.-H. Lee, Non-orthogonal multiple access in coordinated direct and relay transmission. *IEEE Commun. Lett.* **19**(11), 2037–2040 (2015)
5. Z. Zhang, K. Long, A. V. Vasilakos, L. Hanzo, Full-duplex wireless communications: challenges, solutions, and future research directions. *Proc. IEEE.* **104**(7), 1369–1409 (2016)
6. G. Liu, F. R. Yu, H. Ji, V. C. Leung, X. Li, In-band full-duplex relaying: a survey, research issues and challenges. *IEEE Commun. Surv. Tutor.* **17**(2), 500–524 (2015)
7. J.-B. Kim, I.-H. Lee, Capacity analysis of cooperative relaying systems using non-orthogonal multiple access. *IEEE Commun. Lett.* **19**(11), 1949–1952 (2015)
8. L. Yuanwei, D. Zhiguo, E. Maged, P. H. Vincent, Cooperative non-orthogonal multiple access with simultaneous wireless information and power transfer. *IEEE J. Sel. Areas Commun.* **34**(4), 938–953 (2016)
9. S. Lee, D. B. Costa, T. Q. Duong, in *Proceedings IEEE 27th Annual International Symposium*. Outage probability of non-orthogonal multiple access schemes with partial relay selection, Personal, Indoor, and Mobile Radio Communications (PIMRC), (Valencia, 2016), pp. 1–6
10. S. Lee, et al., Non-orthogonal multiple access schemes with partial relay selection. *IET Commun.* **11**(6), 846–854 (2016)
11. Z. Ding, M. Peng, H. V. Poor, Cooperative non-orthogonal multiple access in 5G systems. *IEEE Commun. Lett.* **19**(8), 1462–1465 (2015)
12. P. Xu, et al., Optimal relay selection schemes for cooperative NOMA. *IEEE Trans. Veh. Technol.* **67**(8), 7851–7855 (2018)
13. J. Zhao, et al., Dual relay selection for cooperative NOMA with distributed space time coding. *IEEE Access.* **6**, 20440–20450 (2018)
14. Y. Zhou, V. W. S. Wong, R. Schober, Dynamic decode-and-forward based cooperative NOMA with spatially random users. *IEEE Trans. Wirel. Commun.* **17**(5), 3340–3356 (2018)
15. Md. F. Kader, S. Y. Shin, Coordinated direct and relay transmission using uplink NOMA. *IEEE Wirel. Commun. Lett.* **7**(3), 400–403 (2018)
16. Y. Guo, Y. Li, W. Cheng, H. Zhang, in *IEEE/CIC International Conference on Communications in China (ICCC)*. SWIPT assisted NOMA for coordinated direct and relay transmission, (Beijing, 2018), pp. 111–115
17. Y. Xu, et al., Performance of NOMA-based coordinated direct and relay transmission using dynamic scheme. *IET Commun.* **12**(18), 2231–2242 (2018)
18. X. Yue, et al., Exploiting full/half-duplex user relaying in NOMA systems. *IEEE Trans. Commun.* **66**(2), 560–575 (2018)
19. X. Yue, A. Nallanathan, Y. Liu, S. Kao, Z. Ding, in *IEEE International Conference on Communications (ICC)*. Outage performance of full/half-duplex user relaying in NOMA systems, (Paris, 2017), pp. 1–6
20. X. Yue, Y. Liu, L. Rongke, A. Nallanathan, Z. Ding, in *IEEE Global Communications Conference*. Full/half-duplex relay selection for cooperative NOMA networks, (Singapore, 2017), pp. 1–6
21. N. T. Tan, T. M. Hoang, B. C. Nguyen, in *International Conference on Engineering Research and Applications*. Outage analysis of downlink NOMA full-duplex relay networks with RF energy harvesting over Nakagami-m fading channel (Springer, Cham, 2018), pp. 477–487
22. C. Zhong, Z. Zhang, Non-orthogonal multiple access with cooperative full-duplex relaying. *IEEE Commun. Lett.* **20**(12), 2478–2481 (2016)
23. T. M. C. Chu, H. J. Zepernick, Performance of a non-orthogonal multiple access system with full-duplex relaying. *IEEE Commun. Lett.* **22**(1), 2084–2087 (2018)
24. X.-X. Nguyen, D. T. Do, System performance of cooperative NOMA with full-duplex relay over Nakagami-m fading channels. *Mob. Informa. Syst.* (2019). <https://doi.org/10.1155/2019/7547431>
25. X.-N. Tran, in *3rd International Conference on Recent Advances in Signal Processing, Telecommunications and Computing (SigTelCom)*. Performance of cooperative NOMA system with a full-duplex relay over Nakagami-m fading channels (IEEE, 2019). <https://doi.org/10.1109/sigtelcom.2019.8696186>
26. M. B. Shahab, S. Y. Shin, Time shared half/full-duplex cooperative NOMA with clustered cell edge users. *IEEE Commun. Lett.* **22**(9), 1794–1797 (2018)
27. A. Goldsmith, *Wireless communications*. (Cambridge university press, 2005)
28. E. Everett, et al., in *IEEE Conference Record of the Forty Fifth Asilomar Conference on Signals, Systems and Computers (ASILOMAR)*. Empowering full-duplex wireless communication by exploiting directional diversity, (2011), pp. 2002–2006. <https://doi.org/10.1109/acssc.2011.6190376>
29. D. Bharadia, E. McMillin, S. Katti, Full duplex radios. *ACM SIGCOMM Comput. Commun. Rev.* **43**(4), 375–386 (2013)

30. M. A. Khojastepour, et al., in *Proceedings of the 10th ACM Workshop on Hot Topics in Networks*. The case for antenna cancellation for scalable full-duplex wireless communications, vol. 17 (ACM, 2011). <https://doi.org/10.1145/2070562.2070579>
31. M. Duarte, C. Dick, S. Ashutosh, Experiment-driven characterization of full-duplex wireless systems. *IEEE Trans. Wirel. Commun.* **11**, 4296–4307 (2012)
32. E. Everett, et al., in *Proceedings 49th AACC*. Self-interference cancellation in multi-hop full-duplex networks via structured signaling (IEEE, Monticello, 2011), pp. 1619–1626
33. M. Jain, et al., in *Proceedings of the 17th annual international conference on Mobile computing and networking*. Practical, real-time, full duplex wireless (ACM, 2011), pp. 301–312. <https://doi.org/10.1145/2030613.2030647>
34. S. Hong, et al., Applications of self-interference cancellation in 5G and beyond. *IEEE Commun. Mag.* **52**(2), 114–121 (2014)
35. Z. Zhang, et al., Full duplex techniques for 5G networks: self-interference cancellation, protocol design, and relay selection. *IEEE Commun. Mag.* **53**(5), 128–137 (2015)
36. A. Sabharwal, et al., In-band full-duplex wireless: challenges and opportunities. *IEEE J. Sel. Areas Commun.* **32**(9), 1637–1652 (2014)
37. E. Everett, S. Achaleshwar, S. Ashutosh, Passive self-interference suppression for full-duplex infrastructure nodes. *IEEE Trans. Wirel. Commun.* **13**(2), 680–694 (2014)
38. Y. Wang, et al., Relay selection of full-duplex decode-and-forward relaying over Nakagami-m fading channels. *IET Commun.* **10**(2), 170–179 (2016)
39. L. J. Rodriguez, et al., Optimal power allocation and capacity of full-duplex AF relaying under residual self-interference. *IEEE Wirel. Commun. Lett.* **3**(2), 233–236 (2014)
40. I. S. Gradshteyn, I. M. Ryzhik, *Table of integrals, series, and products*, 6th edn. (Academic Press, New York, 2000)
41. E. Hildebrand, *Introduction to numerical analysis*. (Dover, New York, 1987)

Publisher's Note

Springer Nature remains neutral with regard to jurisdictional claims in published maps and institutional affiliations.

Submit your manuscript to a SpringerOpen[®] journal and benefit from:

- Convenient online submission
- Rigorous peer review
- Open access: articles freely available online
- High visibility within the field
- Retaining the copyright to your article

Submit your next manuscript at ► [springeropen.com](https://www.springeropen.com)
